OFFICE OF NAVAL RESEARCH

GRANT or CONTRACT N00014-90-J-1161

R &T Code 4133030

Technical Report No. 022
Robert J. Nowak

Voltammetric and Amperometric Probes for Single Cell Analysis

by

A. G. Ewing, T. K. Chen

Prepared for Publication

in

Neuromethods: In-Vivo Monitoring I
R. Adams, ed., Human Press
Clifton, NJ

Department of Chemistry
Penn State University
University Park, PA 16802

March 26, 1993

REPORT DOCUMENTATION PAGE

Form Approved
OMB No. 0704-0188

1. AGENCY USE ONLY (Leave blank)	2. REPORT DATE	3. REPORT TYPE AND DATES COVERED
	March 26, 1993	Technical

4. TITLE AND SUBTITLE

Voltammetric and Amperometric Probes for Single Cell Analysis

5. FUNDING NUMBERS

N00014-90-J-1161

6. AUTHOR(S)

A. G. Ewing, T. K. Chen

7. PERFORMING ORGANIZATION NAME(S) AND ADDRESS(ES)

Department of Chemistry
Penn State University
Univerity Park, PA 16802

8. PERFORMING ORGANIZATION REPORT NUMBER

No. 022

9. SPONSORING/MONITORING AGENCY NAME(S) AND ADDRESS(ES)

Office of Naval Research
800 N. Quincy
Arlington, VA 22217-5000

10. SPONSORING/MONITORING AGENCY REPORT NUMBER

11. SUPPLEMENTARY NOTES

Prepared for Publication in Neuromethods: In-Vivo Monitoring I
R. Adams, Ed., Human Press, Clifton, NJ(1994)

12a. DISTRIBUTION AVAILABILITY STATEMENT

Unclassified

12b. DISTRIBUTION CODE

13. ABSTRACT *(Maximum 200 words)*

The use of voltammetry and amperometry to monitor chemical dynamics at single nerve cells and nerve cell model systems has provided information about intracellular neurotransmitter dynamics and a means to directly monitor exocytosis. It is important, however, to emphasize that these techniques can as yet be used only for easily oxidized neurotransmitters and concentration sensitivity is an issue. It is not yet possible to voltammetrically detect submicromolar levels of catecholamine in the cytoplasm of a cell. Finally, these techniques have as yet only been used on cells in culture and large identified cells in invertebrates. A large step in technology is needed to fabricate smaller electrode sizes and manipulation techniques before voltammetric measurements will be made in individual synapses.

14. SUBJECT TERMS

voltammetry and amperometry to monitor chemical dynamics at single nerve cells, intracellular neurotransmitter dynamics, exocytosis

15. NUMBER OF PAGES

61

16. PRICE CODE

17. SECURITY CLASSIFICATION OF REPORT	18. SECURITY CLASSIFICATION OF THIS PAGE	19. SECURITY CLASSIFICATION OF ABSTRACT	20. LIMITATION OF ABSTR/
		unclassified	

VOLTAMMETRIC AND AMPEROMETRIC PROBES FOR SINGLE CELL ANALYSIS

Andrew G. Ewing and Ta Kung Chen
152 Davey Laboratory
Department of Chemistry
Penn State University
University Park, PA 16802
(814) 863-4653
Fax: (814) 863-8081

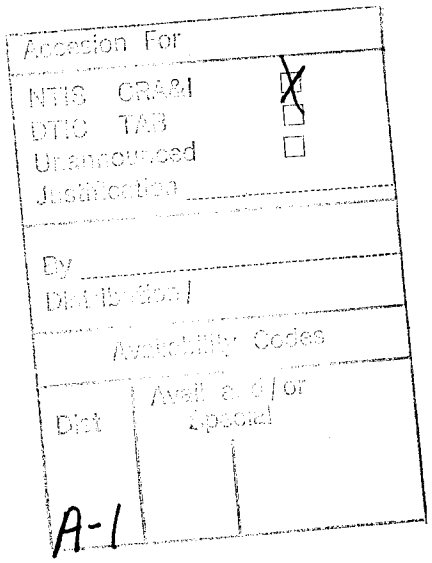

Table of Contents

VOLTAMMETRIC AND AMPEROMETRIC PROBES FOR SINGLE CELL ANALYSIS

1. INTRODUCTION

Chemical analysis of single cells is an area of great interest in the biological and medical sciences. Knowledge of the chemical composition and dynamics of single nerve cells should lead to better models of the cellular neurotransmission process. Information of this type promises to advance our knowledge of neurotransmitter storage, exocytosis and the physiological effects of external stimuli such as drugs and toxins. Advances in these areas require the development of analytical methods capable of monitoring neurotransmitter dynamics at the single cell and subcellular levels.

The considerable interest in studying single cell chemistry has resulted in the development of a number of analytical techniques. These include enzyme activity measurements (Giachobini, 1968), immunoassay (Giachobini, 1987; Ishikawa et al., 1990), microgel electrophoresis (Matioli and Niewisch, 1965), fluorescence imaging techniques (Tank et al., 1988), microscale ion-selective electrodes (Nicholson and Rice, 1988; Amman, 1986), microcolumn separation techniques (Kennedy et al., 1989; Ewing et al., 1992; Hogan and Yeung, 1992), optical and electron microscope techniques (Sossin and Scheller, 1989; Betzig et al., 1991), and secondary ion mass spectrometry (Mantus et al., 1991). Although these methods have provided valuable information, they have important limitations. Most suffer from either inadequate sensitivity, poor quantitative capabilities or an inability to monitor chemical dynamics on a time scale similar to the neurotransmission process.

Voltammetric microelectrodes (Wightman, 1981; 1988; Wightman and Wipf, 1988) are ideally suited for monitoring dynamic chemical changes resulting from discrete neurochemical events as they possess rapid response times. Furthermore, many neurochemicals are easily oxidized. To date, voltammetric microelectrodes have been used to monitor dynamics of catecholamine neurotransmitters both inside single cell cytoplasm and outside single nerve cells (Ewing et al., 1992). The latter experiments have led to the first direct, real-time chemical monitoring of exocytosis and neurotransmitter reverse transport.

Voltammetric microelectrodes used for monitoring single cell neurochemistry have generally been constructed using carbon as the electrode material and have ranged in tip size from 10 or 50 micrometers down to 400 nanometers. These electrodes and pretreatment procedures were discussed in Chapter X [McCreery Chapter].

This chapter describes the use of voltammetric microelectrodes for analysis of neurotransmitter dynamics in and at single nerve cells. The small size of the single cell environment requires extremely small electrodes be used. In addition, as many of these systems involve monitoring model systems in culture, the problem of electrode fouling by components in the cell culture medium must be addressed. Electrode characterization and application to single cell neurochemical dynamics are discussed.

2. INTRACELLULAR VOLTAMMETRY IN INVERTEBRATES

Direct measurements of neurotransmitter and drug concentrations inside single nerve cells can provide unique information concerning the dynamics of drug action, and

neurotransmitter storage and dynamics. Intracellular measurement of cell membrane potential (Parsons et al., 1983) and inorganic ion concentration (Thomas and Moody, 1980) are possible with ultrasmall glass pipettes filled with a saline solution or a liquid ion exchanger, respectively. Voltammetric electrodes small enough to be placed inside single cells while maintaining cell viability have been developed (Meulemans et al., 1986; 1987; Chien et al., 1988; 1990). In this section of this chapter, the application of voltammetry to measurements in the cytoplasm of single nerve cells will be discussed.

2.1. Intracellular Voltammetry with Polished Carbon Fiber Electrodes.

Electrodes with tip diameters of 0.5 to 2 μm have been constructed by electropolishing carbon fibers and then sealing the polished tips in glass. These electrodes have been used to monitor metronidazole, a widely used antibiotic, and antipyrine, an antipyretic drug, in the cytoplasm of identified neurons of *Aplysia californica* (Meulemans et al., 1986). Identified neurons (150-300 μm diameter) of the buccal ganglia were used. Differential pulse voltammetry was used to monitor the concentrations of these two drugs and ascorbic acid as a function of penetration into the cell and the subsequent clearance process. These electrodes were capable of following intracellular drug concentration for periods of 30 to 40 min.

2.2 Intracellular Voltammetry with Platinum and Platinum-Coated Electrodes.

Platinum electrodes with micrometer tip dimensions have also been constructed by electropolishing platinum microwires and sealing the tips in glass as discussed above for carbon. Differential pulse voltammetry has been used to monitor endogenous serotonin injected into cells in the buccal ganglion of *Aplysia californica* and to monitor free levels

of serotonin in single cell cytoplasm following cell stimulation or extracellular application of L-tryptophan, reserpine or p-chlorophenylalanine (Meulemans et al., 1987). Differential pulse voltammograms obtained in an *Aplysia neuron* are shown in Figure 1. Voltammograms in the background buffer and in the cytoplasm of single cholinergic neurons showed no peak for serotonin, whereas, a distinct serotonin peak is observed in the metacerebral neuron. This was confirmed by injecting serotonin into the cell body of this neuron and observing an increase in the voltammetric peak. The increase in serotonin persisted for approximately 10 min and the endogenous level of serotonin measurements agree with estimates of cytoplasmic serotonin in this cell obtained with fluorescent (McCaman et al., 1973)) and radioenzymatic (Brownstein et al., 1974) assays.

Intracellular voltammetry has been used in the metacerebral neuron to investigate the effect of cell stimulation on intracellular serotonin levels (Meulemans et al., 1987). Figure 2 shows the levels of serotonin recorded with differential pulse voltammetry during stimulation by direct intracellular depolarization of the soma and by application of extracellular potassium chloride. It was speculated that cell stimulation likely leads to increased serotonin synthesis resulting in the increased cytoplasmic levels. If this is true in terminals also, this might be very important in the regulation of transmitter availability and synaptic efficacy.

2.3 Intracellular Voltammetry with Carbon Ring Electrodes.

Electrodes with tip diameters as small as 1 μm have been fabricated using hydrocarbon pyrolysis inside silica microcapillaries (Kim et al., 1986; Chien et al., 1988). Methane is pyrolyzed inside silica micro capillaries at temperatures below the silica

melting point leaving a conductive film of pyrolytic carbon inside the capillary tip. Cleaving the epoxy-filled tip with a scalpel exposes a ring of carbon.

The intracellular response of ultrasmall carbon and platinum ring electrodes has been investigated (Lau et al., 1991; Chen et al., 1992). Adsorption of high molecular weight species on the electrode surface appears to result in deterioration of the amperometric signal. An analytical method has been developed to allow quantitative voltammetry to be obtained (Lau et al., 1991). This method assumes that there is a linear dependence between the degree of electrode fouling of carbon ring electrodes and the number of scans taken in the neuronal microenvironment during intracellular voltammetry.

The left pedal ganglion of the pond snail *Planorbis corneus* contains a single large dopamine neuron that closely resembles mammalian neurons in several ways (Osborne et al., 1975). It displays nomifensine-sensitive dopamine uptake, reserpine-sensitive vesicular storage of dopamine, and metabolizes dopamine to dihydroxyphenylacetic acid. However, unlike mammalian dopamine neurons it is approximately 200 μm in diameter facilitating single cell analysis. In addition, this cell lacks ascorbic acid, allowing the unambiguous electrochemical detection of dopamine.

Carbon ring electrodes have been used to monitor dopamine levels in the cytoplasm of the large dopamine cell located on the left Pedal ganglion of the pond snail, *Planorbis corneus* (Chien et al., 1988; 1990; Lau et al., 1991). A schematic of the system employed is shown in Figure 3. In these experiments, endogenous levels of dopamine were below the detection limit of the electrodes (approx. 3 μM), which is considerably below the cytoplasmic levels of serotonin observed in the metacerebral neuron of *Aplysia*

(Meulemans et al., 1987). Cytoplasmic levels of dopamine could, however, be increased to detectable levels by external application of ethanol or exogenous dopamine. Figure 4 shows the electrochemical response of an electrode placed in the cytoplasm of the dopamine cell following external application of dopamine before and after nomifensine. Nomifensine, a competitive inhibitor of the dopamine transporter, clearly reduces the amount of dopamine entering the cell in this experiment.

In addition to monitoring intracellular dopamine, carbon ring electrodes have been coated with platinum and platinum with glucose oxidase to monitor intracellular oxygen levels (Lau et al., 1992) and intracellular glucose transients (Abe et al., 1991; 1992), respectively. The intracellular level of oxygen was estimated at 32 μM in the identified dopamine neuron of *Planorbis corneus*. Changes in intracellular glucose concentration on the order of 0.8 mM have been observed following injection of exogenous glucose into the cell.

3. EXTRACELLULAR VOLTAMMETRY AT SINGLE CELLS

Direct measurements of neurotransmitters outside single neurons can provide unique information about dynamic processes including neurotransmitter transport and exocytosis. This section deals with electrochemical measurements to monitor catecholamine dynamics outside single cells. Both operation of the dopamine transporter in reverse (reverse transport) and exocytosis of catecholamines have been observed with this methodology.

3.1 Reverse Transport of Dopamine from the Cell Body of *Planorbis corneus*.

Voltammetry can be used to monitor dopamine levels both inside and outside single nerve cells. As shown above, intracellular voltammetry can be used to monitor dopamine transport into the cell body of the identified dopamine neuron of *Planorbis corneus*. Likewise, a carbon ring electrode placed immediately outside the cell body of this neuron can be used to monitor the same transporter operating in reverse. Injection of dopamine into the cytoplasm of the dopamine neuron leads to a rapid release of dopamine that is nomifensine sensitive (Figure 5). Since nomifensine blocks substrate flux across the plasma membrane via the dopamine transporter, this suggests that most dopamine release following intracellular injection occurs via reverse transport.

Measurement of reverse transport has been used to study the mechanism of action of amphetamine. The actions of amphetamine at the cellular level have been controversial and have included mechanisms involving blocking catecholamine transport across the plasma membrane and also involving vesicular storage of catecholamine. Injection of amphetamine directly into the cytoplasm of the identified dopamine neuron on *Planorbis corneus*, which bypasses the uptake transporter, causes dopamine release (Figure 6). In these experiments, carbon ring electrodes were used to measure dopamine concentrations immediately outside the cell body following an injection of 8 pL of 100 mM d-Amph into the cell. Based on an estimated cell volume of 8 nL, this resulted in an intracellular level of 100 μM. Extracellular dopamine increased to a maximal level 14 s following the injection. The shape of the voltammogram obtained at the peak current value closely matched the voltammogram of a dopamine standard and showed that extracellular

dopamine reached about 1.6 μM following the amphetamine injection. Combined with evidence for specific uptake of amphetamine (Zaczek, 1991) and the ability of amphetamine to release catecholamines from isolated vesicles (Sulzer and Rayport, 1990), these observations indicated that, at least in part, amphetamine releases dopamine via an intracellular action.

3.2 Monitoring Single Exocytotic Events.

Secretion of catecholamines from single exocytotic events has been monitored by use of carbon fiber electrodes placed against the outside of the plasma membrane of bovine adrenal medullary chromaffin cells in primary culture (Leszczyszyn et al., 1990; 1991; Wightman et al., 1991; Chow et al., 1992). These cells were stimulated with nicotine via a microinjection pipette and a pressure injection system while simultaneously monitoring catecholamines with the small electrode (Figure 7). The response to this stimulation was monitored with voltammetry repeated every 100 ms (Figure 8). When norepinephrine is ejected from the micropipette as a control, the current at the electrode increases momentarily and then returns to baseline over a period of 10 to 20 s (Figure 8C). However, nicotine stimulation results in numerous current transients that are in fact chemical spikes from the cell (Figure 8D). Voltammograms obtained for authentic norepinephrine are similar to those corresponding to the current transients observed (Figure 8A and B). The current rise under the transients observed in these preliminary experiments might be the result of an overall increase in the extracellular concentration of catecholamine or it might be an artifact of the nicotine ejection. Later experiments with lower nicotine concentrations have shown much smaller changes in the baseline current

(Wightman et al., 1991). Initial estimates of the number of catecholamine molecules in each current transient have assumed that all the released catecholamine is oxidized. Using Faraday's law to calculate the amount of catecholamine released, 5 to 10 amol of catecholamine is released in each exocytotic event (Leszczyszyn et al., 1990; 1991; Wightman et al., 1991).

The effect of different secretagogues on the release of catecholamines from adrenal cells has been examined (Wightman et al., 1991). Ejection of nanoliter volumes of 100 μM nicotine or 1 mM carbamoylcholine leads to release of catecholamines characterized by a broad envelope under the transients with a concentration greater than 10 μM (Wightman et al., 1991). When cells are stimulated with only 10 μM nicotine or 60 mM KCl, this envelope is significantly less. Following 10 μM nicotine or 60 mM KCl, the envelope is 23% or 22%, respectively, of that following 100 μM nicotine. In addition, the frequency of exocytotic events decreases from 1.2 ± 0.2 Hz to 0.5 ± 0.2 Hz and 0.6 ± 0.2 Hz, respectively. Histograms of the areas of the electrochemical responses shown, however, are similar for all the secretagogues (Figure 9). It is interesting to note that the distribution of spike areas is clearly skewed for all the secretagogues suggesting that a distribution of granule content is present in each cell.

Adrenal medullary chromaffin cells in culture present an excellent model system to study neurosecretion (Trifaro and Lee, 1980). However, there are clearly at least two subpopulations of cells that secrete either norepinephrine or epinephrine. In fact, microcolumn liquid chromatography of single adrenal cells has shown that these cells can contain either predominantly norepinephrine, epinephrine or a high level of both (Cooper

et al., 1992). Despite their structural similarity, voltammetry at microelectrodes can be used to discriminate between norepinephrine and epinephrine by monitoring the rate of internal cyclization following oxidation (Hawley et al., 1967). This cyclization reaction leads to the formation of an adrenochrome which can be detected as an additional voltammetric wave on the negative-going scan of the cyclic voltammogram (Ciolkowski et al., 1992). This is shown in Figures 10 and 11 for current traces obtained by voltammetry at two different adrenal cells with epinephrine released from one cell (Figure 10) and norepinephrine released from the other cell (Figure 11). In these experiments, approximately 75% of the cells examined released only epinephrine or norepinephrine, whereas 25% of the cells released both catecholamines in response to a 100 μM nicotine simulus. It appears that these cells release catecholamine in the same proportions that they store catecholamines.

Single exocytotic events can also be monitored by voltammetry at adrenal cells following permeabilization with digitonin (Jankowski et al., 1992). Digitonin is commonly used to permeabilize adrenal cells to introduce reagents into the cell (Dunn and Holz, 1983). During digitonin-induced permeabilization, catecholamine secretion can be induced by low levels of calcium ion in the medium surrounding the cells. Voltammetry has been used to monitor the exocytosis of single chromaffin granules from digitonin-permeabilized cells. Strong evidence is given that catecholamine release following digitonin is via exocytosis. This release is calcium dependent and reaches a maximum at calcium concentrations at or above 19 μM. Finally, exocytotic release can be

distinguished from nonexocytotic release by analysis of the shape of the current transients observed at the electrode.

3.3 Delay in Vesicle Fusion Observed by Amperometry.

Whole-cell patch-clamping has been used to examine the delay between adrenal cell stimulation and exocytosis (Chow et al., 1992). Exocytosis is thought to occur on a submillisecond time scale based on measurements of post-synaptic membrane potential following stimulation (Llinas et al., 1981; Edwards et al., 1990). In nonsynaptic cells, the absence of a post-synaptic neuron prevents this type of measurement. Amperometric measurements with microelectrodes provides a means to directly monitor single exocytotic events. When cells are depolarized for 25 ms, exocytosis is observed following highly varied delay times (Figure 12). A histogram of the areas of the amperometric responses and the delay from the initiation of the depolarization to the observed release is shown in Figure 13. Cells were held at -60 mV and depolarized at +10 mV for 25 ms to activate calcium channels. The average spike contained 2 x 10^{-6} catecholamine molecules, although this again follows a skewed distribution similar to that shown above for release following exposure to a secretagogue. The latency period between depolarization and release is usually less than 100 ms and events after this time are approximately constant. Since the exocytosis process in adrenal cells is slow following depolarization (5-100 ms), it is likely that calcium or membrane depolarization trigger a cascade of events that manifests itself later as the exocytosis process. The rationale for the wide variability of the latency times is not yet clear.

In addition to the latency time between depolarization and exocytosis, evidence has also been obtained by amperometry to demonstrate the existence of a fusion pore during exocytosis (Chow et al., 1992). This could represent a slow leakage of catecholamines through a small opening at the initiation of the exocytotic event via a structure similar to a gap junction (Thomas et al., 1988). Figure 13a shows three current transients observed at the electrode following cell depolarization with two of these showing a small rise in current prior to the larger spike. Two-thirds of all current transients observed are preceded by a pre-cise or "foot". Histograms for the duration of this "foot" of the transients are shown in Figures 13b and c. This is the first direct, real-time evidence for the existence of a fusion pore during exocytosis.

3.4 Temporal Characteristics of Exocytosis at Adrenal Cells.

Catecholamine granules in adrenal medullary chromaffin cells are known to contain ascorbic acid, ATP and the protein chromogranin A in addition to catecholamine (Winkler and Westhead, 1980; O'Conner and Frigon, 1984). Dissociation of the intravesicular matrix of these cells has been described as a pH-dependent conformational change of the chromogranin A which binds the catecholamines in an intravesicular matrix (Yoo and Lewis, 1992). Both amperometry and fast-scan cyclic voltammetry have been used to examine the diffusional profile of catecholamine released from individual exocytotic events as a function of distance between the electrode and the cell and of extracellular pH (Schroeder et al., 1992; Jankowski et al., 1993). Taken together the data appear to indicate that catecholamine in adrenal cell granules is bound to chromogranin A and that this chromogranin A is bound to the vesicular membrane at the lower pH that exists in the

granule prior to fusion with the plasma membrane and exposure to the pH 7.5 external medium. Thus a conformational change of chromogranin A during exocytosis appears to be an important step defining the time course of catecholamine release.

3.5 Application of Amperometry to Monitoring the Effects of Autoreceptors.

The release of catecholamines to the extracellular synaptic cleft can be regulated by several factors including presynaptic α_2-autoreceptor activation (Starke, 1981). The released extracellular catecholamines act on presynaptic α_2-autoreceptors to inhibit further catecholamine release (Westfall, 1977; Starke, 1977). Agonists of α_2-autoreceptors such as clonidine or guanfacine cause suppression of locus cell firing and decrease the release of catecholamines (Pelayo et al., 1980; Jackisch et al., 1992), whereas α_2-autoreceptor antagonists such as piperoxan, yohimbine and idazoxan reverse these inhibitory effects and increase release (Dennis et al., 1987; Abercrombie et al., 1988).

Although some experiments have provided evidence about presynaptic mechanisms, it is not always possible to determine if the drugs affect the presynaptic terminals directly, or whether they act primarily on nearby cells which then emit a second signal to the presynaptic terminals. This is particularly difficult to decide in tissue studies. Basically, there are two methods to study the interaction of neurotransmitters or drugs with cells. The first procedure is to determine the biological response of an intact isolated organ, such as the guinea pig ileum, to applied agonists or antagonists. The disadvantage to this procedure lies in the difficulty in discriminating between a large number of processes taking place before the drug interacts with the receptor. The second approach to studying receptors is to measure ligand binding to a homogenate or slice preparation. This

technique became feasible with the development of ligands of a high specific radioactivity and a high affinity for the receptor. Neither of these techniques eliminate post-synaptic effects. The use of amperometric monitoring of catecholamine exocytosis, combined with the application of receptor agonists or antagonists is a new method which can functionally identify autoreceptors directly since there are no postsynaptic cells. The electrochemical measurements described here are spatially resolved to the single cell level because of the size of the microelectrode sensor as well as the small volume of the applied chemical stimulus.

To demonstrate the effect of autoreceptors on exocytosis from adrenal cells, a protocol involving repeated nicotine stimulations of the same cell has been developed (Zhou et al., 1994). Individual cells were repeatedly stimulated with 3-s exposures to 100 μM nicotine at intervals of 100 to 400 s. The current responses for neurohormone secretion were integrated to obtain the total charge for all the current transient responses over a 200-s time window. For repetitive stimulations, the ratio of total secretion of the second to the first exposure is 0.32 ± 0.05 (n=7) and the ratio of the third to the second exposure is 0.80 ± 0.02 (n=4).

The effects of autoreceptors on single adrenal medullary chromaffin cells were examined by 5-s pressure applications of 20 μM piperoxan approximately 80 s after a 3-s exposure to nicotine. Figure 14 shows the response to piperoxan compared to a control experiment. To evaluate the effect of piperoxan on catecholamine exocytosis, the integrated current (large) for all the spikes (release events) following nicotine and piperoxan together has been compared to the total charge for release events after only

nicotine. A 15% (n=3) increase in catecholamine exocytosis is observed after the nicotine and piperoxan compared to a 46% (n=6) decrease in release for the control experiment (identical protocol without application of piperoxan). These data strongly suggest that a negative feedback mechanism exists. Exposure to piperoxan enhances the release of catecholamines from nicotine-stimulated cells; however, piperoxan alone has no effect on release from cells not exposed to nicotine.

Perhaps the most widely known sympathomimetic drug is amphetamine. The actions of amphetamine appear to be manifested as an increased level of extracellular catecholamine in regions of the central nervous system (Zetterström et al., 1983; Hernandez et al., 1987; Sharp et al., 1987). A great deal of work has shown that amphetamine enhances release of catecholamines (Kuczenski, 1983), inhibits the catecholamine transporter (Wise and Bozarth, 1987), and that it accelerates exchange diffusion across the plasma membrane (Fisher and Cho, 1979; Kuczenski, 1983). In addition, recent evidence suggests that amphetamine acts as a weak base to disrupt catecholamine vesicularization and, therefore, enhances the cytoplasmic level of neurotransmitter for subsequent release via reverse transport (Sulzer and Rayport, 1990). All these actions appear to play a role in the neuronal response to amphetamine.

Amphetamine also appears to affect the exocytosis of catecholamine from adrenal cells (Zhou et al., 1994). A 5-s application of 20 μM amphetamine at approximately 20 s after stimulation of an adrenal cell with nicotine results in a dramatic increase in catecholamine release events (Figure 15). Integrating the total current under all the release events and comparing them to a control experiment reveals that amphetamine

results in an 870% increase in exocytosis (n=3). It appears that amphetamine might act as an antagonist of α_2-autoreceptors.

3.6 Amperometric Monitoring of Exocytosis from PC12 Cells.

Mammalian neurons are difficult to work with in the laboratory as they stop proliferation once they have matured. Greene and Tischler established a nerve growth factor responding clonal line of rat pheochromocytoma (PC12) cells in 1976. This cell line shares many physiological properties with primary cultures of symphathetic ganglion neurons (Green and Tischler, 1976; Schubert et al., 1980), and has been studied as a model for the developing sympathetic nerve (Wagner, 1985). PC12 cells can synthesize, store and release catecholamines in a manner similar to sympathetic ganglion neurons (Green and Tischler, 1976; Schubert et al., 1980; Wagner, 1985). They are more similar to sympathetic ganglion neurons than to chromaffin cells, because they contain more dopamine than norepinephrine with no detectable level of epinephrine (Clift-O'Grady et al., 1990). Most importantly, PC12 cell vesicles are valid analogues of brain synaptic vesicles for four criteria: size, density, protein composition, and endocytotic origin (Wagner, 1985; Clift-O'Grady et al., 1990).

Carbon fiber electrodes have been used to monitor single exocytotic events from individual PC12 cells (Chen et al., 1994b). The electrode is placed against the top of a cell in culture and the cell is stimulated in a manner to that described above for adrenal cells with KCl or nicotine. Figure 16 shows the amperometric response following three successive stimulations with both 1 mM nicotine and 105 mM KCl. Stimulated release is not observed from these cells if calcium is omitted from the medium. In addition,

preliminary data suggests that exposure to nicotine alone results in minimal exocytosis and that is only after a substantial delay. Exposure to elevated potassium chloride causes most of the exocytosis observed. Individual current spikes have an average half width of 9.3 ± 0.1 ms (n=1912 from 13 cells) and the average catecholamine level calculated with Faraday's law is 190 zmol (114,000 molecules) per vesicle. A histogram of the amount of catecholamine released per vesicle is shown in Figure 17. This histogram has the same skewed profile as observed for adrenal medullary chromaffin cells; however, the average vesicle content is much lower. The size distribution of vesicles is relatively narrow for PC12 cells with 85% of the release events corresponding to less than 330 zmol. This is an example of the tremedous sensitivity that can be obtained using amperometry to monitor catecholamine exocytosis.

The PC12 system has also been used to examine the effects of amphetamine (Sulzer et al., submitted). As one of the proposed mechanisms of amphetamine is the redistribution of catecholamines from synaptic vesicles to the cytoplasm (Sulzer and Rayport, 1990; Sulzer et al., 1993), one can use voltammetric methods to examine the effects of amphetamine on quantal size. To measure the dopamine content of individual synaptic vesicles, carbon fiber electrodes can be used to detect quantal packets containing as few as 15,000 molecules. Cells were stimulated with 1 mM nicotine in 105 mM KCl (30 nL). Incubation in 10 μM amphetamine for 10 min prior to the stimulation reduced the stimulated catecholamine released per exocytotic event to 48 ± 5.4% of control (n=7 cells) (Figure 18). These results demonstrate that amphetamine can attenuate stimulus-dependent release by reducing quantal size. Quantal analysis studies generally assume that

all vesicles contain a constant level of neurotransmitter. Data shown earlier in this chapter show that considerable variability in the size of release events exists. Here it is demonstrated that quantal size can be pharmacologically manipulated. These data combined suggest that both physiological and pharmacological alterations of quantal size might well play an important role in the modulation of catecholamine release.

3.7 Voltammetric Monitoring of Exocytosis from Cell Bodies.

The cell body of a neuron is generally not thought to be involved in calcium-dependent exocytosis of neurotransmitters. Exocytosis of neurotransmitters is thought to occur at synaptic terminals. In fact, placement of a carbon fiber microelectrode against the cell body of the identified dopamine neuron of *Planorbis corneus* with subsequent stimulation by exposure to KCl results in a massive exocytotic response (Figure 19). This release is calcium dependent and voltammograms obtained during the current transients are nearly identical to those obtained in authentic dopamine (Figure 20). A histogram (Figure 21) of the spike areas again shows the typical skewed shape characteristic of exocytosis of catecholamines shown above for adrenal and PC12 cells. The average vesicle contains 0.8 amol of dopamine with a broad distribution of sizes that is, perhaps, expected for a primitive neuron. Interestingly, the frequency of exocytotic events observed from the *Planorbis* cell does not diminish rapidly as was observed for adrenal cells and PC12 cells. Although exocytosis from this cell does appear to show a bursting pattern, once a cell is stimulated it can undergo rapid exocytosis for minutes to hours. As many as 89,000 release events have been observed from one spot on a cell after a single stimulation.

The dopamine cell used has been estimated to contain 5 pmol of dopamine based on immunofluorescence measurements (Powell and Cottrell, 1974). If virtually all the dopamine is estimated to be bound in vesicles (Chien et al., 1990), this indicates that there must be approximately 6 x 10^6 vesicles in one cell (based on an average 0.8 amol of dopamine per vesicle). Hence 89,000 events represents only 1.5% of the total catecholamine in the cell. This represents the first direct measurement of exocytosis of neurotransmitter from the cell body of a processed neuron.

4. SUMMARY AND FUTURE OUTLOOK

The use of voltammetry and amperometry to monitor chemical dynamics at single nerve cells and nerve cell model systems has provided information about intracellular neurotransmitter dynamics and a means to directly monitor exocytosis. It is important, however, to emphasize that these techniques can as yet be used only for easily oxidized neurotransmitters and concentration sensitivity is an issue. It is not yet possible to voltammetrically detect submicromolar levels of catecholamine in the cytoplasm of a cell. Finally, these techniques have as yet only been used on cells in culture and large identified cells in invertebrates. A large step in technology is needed to fabricate smaller electrode sizes and manipulation techniques before voltammetric measurements will be made in individual synapses. This will be one of the exciting experiments of the future.

ACKNOWLEDGMENTS

We would like to thank our coworkers and colleagues who have contributes to the work in this chapter. The Office of Naval Research, National Science Foundation and the National Institutes of Health supported the work in our laboratory. A.G.E. is a Camille and Henry Dreyfus Teacher-Scholar.

REFERENCES

Abe, T., Lau, Y. Y., and Ewing, A. G. (1991) Intracellular Analysis With an Immobilized-Enzyme Glucose Electrode Having a 2-μm Diameter and Subsecond Response Time. *J. Am. Chem. Soc.* **113,** 7421-7423.

Abe, T., Lau, Y. Y., and Ewing, A. G. (1992) Characterization of Glucose Microsensors for Intracellular Measurements. *Anal. Chem.* **64,** 2160-2163.

Abercrombie, E. D., Keller, R. M., and Zigmond, M. J. (1988) Characterization of Hippocampal Norepinephrine Release as Measured by Microdialysis Perfusion: Pharmacological and Behavioral Studies. *Neuroscience* **27,** 897-904.

Amman, D. (1986) *Ion Selective Microelectrodes*. Springer-Verlag, Berlin.

Betzig, E., Trautman, J. K., Harris, T. D., Weiner, J. S., and Kostelak, R. L. (1991) Breaking the Diffraction Barrier: Optical Microscopy on a Nanometric Scale. *Science* **251,** 1468-1470.

Brownstein, M. J., Saavedra, J. M., Axelrod, J., Zeman, C. H., and Carpenter, D. O. (1974) Coexistence of Several Putative Neurotransmitters in Single Identified Neurons of Aplysia. *Proc. Natl. Acad. Sci. U.S.A.* **71,** 4662-4665.

Chen, T. K., Lau, Y. Y., Wong, D. K. Y., and Ewing, A. G. (1992) Pulse Voltammetry in Single Cells Using Platinum Microelectrodes. *Anal. Chem.* **64,** 1264-1268.

Chen, G., Luo, G. and Ewing, A. G. ((1994a) Exocytosis of Neuromessengers from Nerve Cell Bodies Revealed by Electrochemical Monitoring of Single Secretory Events. submitted to *Nature*.

Chen, T.-K., Luo, G., and Ewing, A. G. (1994b) Amperometric Monitoring of Stimulated Catecholamine Quantal Release from Rat Pheochromocytoma (PC12) Cells at the Zeptomole Level. submitted to *Anal. Chem.*

Chien, J. B., Saraceno, R. A., and Ewing, A. G. (1988) Intracellular Voltammetry with Ultrasmall Carbon Ring Electrodes. in *Redox Chemistry and Interfacial Behavior of Biological Molecules*. (Dryhurst, G. and Niki, K., eds.) pp. 417-424, Plenum Pub. Corp., NY.

Chien, J. B., Wallingford, R. A., and Ewing, A. G. (1990) Estimation of Free Dopamine in the Cytoplasm of the Giant Dopamine Cell of *Planorbis corneus* by Voltammetry and Capillary Electrophoresis. *J. Neurochem.* **54**, 633-638.

Chow, R. H., von Rüden, L., and Neher, E. (1992) Delay in Vesicle Fusion Revealed by Electrochemical Monitoring of Single Secretory Events in Adrenal Chromaffin Cells. *Nature* **356,** 60-63.

Ciolkowski, E. L., Cooper, B. R., Jankowski, J. A., Jorgenson, J. W., and Wightman, R. M. (1992) Direct Observation of Epinephrine and Norepinephrine Cosecretion from Individual Adrenal Medullary Chromaffin Cells. *J. Am. Chem. Soc.* **114,** 2815-2821.

Clift-O'Grady, L., Linstedt, A. D., Lowe, A. W., Grote, E., and Kelly, R. B. (1990) Biogenesis of Synaptic Vesicle-Like Structures in a Pheochromocytoma Cell Line, *J. Cell. Biol.* **110,** 1693-1703.

Cooper, B. R., Jankowski, J. A., Leszczyszyn, D. J., Wightman, R. M., and Jorgenson, J. W. (1992) Quantitative Determination of Catecholamines in Individual Bovine

Adrenomedullary Cells by Reverse-Phase Microcolumn Liquid Chromatography with Electrochemical Detection. *Anal. Chem.* **64,** 691-694.

Dennis, T., L'Heureux, R., Carter, C., and Scatton, B. (1987) Presynaptic α_2-adrenoreceptors Play a Major Role in the Effects of Idazoxan on Cortical Noradrenaline Release (As Measured by In Vivo Dialysis) in the Rat. *J. Pharmacol. Exp. Ther.* **241,** 642-649.

Dunn, L. A. and Holz, R. W. (1983) Catecholamine Secretion from Digitonin-Treated Adrenal Medullary Chromaffin Cells. *J. Biol. Chem.* **258,** 4989-4993.

Edwards, F. A., Konnerth, A., and Sakmann, B. (1990) Quantal Analysis of Inhibitory Synaptic Transmission In the Dentate Gyrus of Rat Hippocampal Slice: A Patch-Clamp Study. *J. Physiol.* **430,** 213-249.

Ewing, A. G., Strein, T. G., and Lau, Y. Y. (1992) Analytical Chemistry in Microenvironments: Single Nerve Cells. *Accts. Chem. Res.* **25,** 440-447.

Fischer, J. F. and Cho, A. K. (1979) Chemical Release of Dopamine from Striatal Homogenates: Evidence for an Exchange Diffusion Model. *J. Pharmac. Exp. Ther.* **208,** 203-209.

Giacobini, E. (1968) Chemical Studies on Individual Neurons (I) Vertebrate Nerves. *Neurosci. Res.* **1,** 1-71.

Giacobini, E. (1987) Neurochemical Analysis of Single Neurons. *J. Neurosci. Res.* **18,** 632-637.

Green, L. A. and Tischler, A. S. (1976) Establishment of a Noradrenergic Clonal Line of Rat Adrenal Pheochromocytoma Cells Which Respond to Nerve Growth Factor. *Proc. Natl. Acad. Sci. U.S.A.* **73,** 2424-2428.

Hawley, M. D., Tatawawadi, S. V., Piekarski, S., and Adams, R. N. (1967) Electrochemical Studies of the Oxidation Pathway of Catecholamines. *J. Am. Chem. Soc.* **89,** 447-450.

Hernandez, L., Lee, F., and Hoebel, B. G. (1987) Simultaneous Microdialysis and Amphetamine Infusion in the Nuleus Accumbens and Striatum of Freely Moving Rats: Increase in Extracellular Dopamine and Serotonin. *Brain Res. Bull.* **19,** 623-628.

Hogan, B. L. and Yeung, E. S. (1992) Determination of Intracellular Species at the Level of a Single Erythrocyte via Capillary Electrophoresis with Direct and Indirect Fluorescence Detection. *Anal. Chem.* **64,** 2841-2845.

Ishikawa, E., Hashida, S., Kohno, T., and Hirota, K. (1990) Ultrasensitive Enzyme Immunoassay. *Clin. Chim. Acta* **194,** 51-72.

Jackisch, R., Huang, H. Y., Rensing, H., Lauth, D., Allgaier, C., and Hertting, G. (1992) α_2-Adrenoceptor Mediated Inhibition of Exocytotic Noradrenaline Release in the Absence of Extracellular Calcium. *Eur. J. Pharamcology Molecular Pharmacology Section* **8(3),** 245-252.

Jankowski, J. A., Schroeder ,T. J., Ciolkowski, E. L., and Wightman, R. M. (1993) Temporal Characteristics of Quantal Secretion of Catecholamines from Adrenal Medullary Cells. *J. Biol. Chem.* **268,** 14694-14700.

Jankowski, J. A., Schroeder, T. J., Holz, R. W., and Wightman, R. M. (1992) Quantal Secretion of Catecholamines Measured from Individual Bovine Adrenal Medullary Cells Permeabilized with Digitonin. *J. Biol. Chem.* **267,** 18329-18335.

Kennedy, R. T., Oates, M. D., Cooper, B. R. Nickerson, B., and Jorgenson, J. W. (1989) Microcolumn Separations and the Analysis of Single Cells. *Science* **246,** 57-63.

Kim, Y.-T., Scarnulis, D. M., and Ewing, A. G. (1986) Carbon-Ring Electrodes with 1-μm Tip Diameter. *Anal. Chem.* **58,** 1782-1786.

Kuczenski, R. (1983) Biochemical Actions of Amphetamine and Other Stimulants. in *Stimulants: Neurochemical, Behavioral, and Clinical Perspectives* (Creese, I., ed.) pp. 31-61, Raven Press, NY.

Lau, Y. Y., Abe, T., and Ewing, A. G. (1992) Voltammetric Measurement of Oxygen in Single Neurons Using Platinized Carbon Ring Electrodes. *Anal. Chem.* **64,** 1702-1705.

Lau, Y. Y., Chien, J. B., Wong, D. K. Y., and Ewing, A. G. (1991) Characterization of the Voltammetric Response at Intracellular Carbon Ring Electrodes. *Electroanalysis* **3,** 87-95.

Leszczyszyn, D. J., Jankowski, J. A., Viveros, O. H., Diliberto, Jr., E. J., Near, J. A., and Wightman, R. M. (1990) Nicotinic Receptor-Mediated Catecholamine Secretion from Individual Chromaffin Cells. *J. Biol. Chem.* **265,** 14736-14737.

Leszczyszyn, D. J., Jankowski, J. A., Viveros, O. H., Diliberto, Jr., E. J., Near, J. A., and Wightman, R. M. (1991) Secretion of Catecholamines from Individual Adrenal Medullary Chromaffin Cells. *J. Neurochem.* **56,** 1855-1863.

Llinas, R., Steinberg, I. Z., and Walton, K. (1981) Relationship Between Presynaptic Calcium Current and Postsynaptic Potential in Squid Giant Synapse. *Biophys. J.* **33,** 323-352.

Mantus, D. S., Valaskovic, G. A., and Morrison, G. H. (1991) High Mass Resolution Secondary Ion Mass Spectrometry via Simultaneous Detection with a Charge Coupled Device. *Anal. Chem.* **63,** 788-792.

Matioli, G. T. and Niewisch, H. B. (1965) Electrophoresis of Hemoglobin in Single Erythrocytes. *Science* **150,** 1824-1826.

McCaman, M. W., Weinreich, D., and McCaman, R. E. (1973) The Determination of Picomole Levels of 5-Hydroxytryptamine and Dopamine in Aplysia, Tritonia and Leech Nervous Tissues. *Brain Res.* **53,** 129-137.

Meulemans, A., Poulain, B., Baux, G., and Tauc, L. (1987) Changes in Serotonin Concentration in a Living Neurone: A Study by On-Line Intracellular Voltammetry. *Brain Res.* **414,** 158-162.

Meulemans, A., Poulain, B., Baux, G., Tauc, L., and Henzel, D. (1986) Micro Carbon Electrodes for Intracellular Voltammetry. *Anal. Chem.* **58,** 2088-2091.

Nicholson, C. and Rice, M. E. (1988) Use of Ion-Selective Microelectrodes and Voltammetric Microsensors to Study Brain Cell Microenvironment. in *Neuromethods: Neuronal Microenvironment* (Boulton, A. A., Baker, G. B., and Walz, W., eds.) pp. 247-361, Humana Press, Clifton, NJ.

O'Connor, D. T. and Frigon, R. P. (1984) Chromogranin A, The Major Catecholamine Storage Vesicle Soluble Protein. *J. Biol. Chem.* **259,** 3237-3247.

Osborne, N. N., Priggemeier, E., and Neuhoff, V. (1975) Dopamine Metabolism in Characterized Neurones of *Planorbis corneus*. *Brain Res.* **90,** 261-271.

Parsons, D. W., Maat, A. T., and Pinsker, H. M. (1983) Selective Recording and Stimulation of Individual Identified Neurons in Freely Behaving Aplysia. *Science* **221,** 1203-1206.

Pelayo, F., Dubocovich, M. L., and Langer, S. Z. (1980) Inhibition of Neuronal Uptake Reduces the Presynaptic Effects of Clonidine but not of α_2-Methylnoradrenaline on the Stimulation-Evoked Release of ^{3}H-Noradrenaline from Rat Occipital Cortex Slices. *Eur. J. Pharmacol.* **64,** 143-155.

Powell, B. and Cottrell, G. A. (1974) Dopamine in an Identified Neuron of *Planorbis corneus*. *J. Neurochem.* **22,** 605-606.

Schroeder, T. J., Jankowski, J. A., Kawagoe, K. T., Wightman, R. M., Lefrou, C., and Amatore, C. (1992) Analysis of Diffusional Broadening of Vesicular Packets of Catecholamines Released from Biological Cells During Exocytosis. *Anal. Chem.* **64,** 3077-3083.

Schubert, D., LaCorbiere, M., Klier, F. G., and Steinbach, J. H. (1980) The Modulation of Neurotransmitter Synthesis by Steroid Hormones and Insulin. *Brain Res.* **190,** 67-79.

Sharp, T., Zetterström, T., Ljungbers, T., and Ungerstedt, U. (1987) A Direct Comparison of Amphetamine-Induced Behaviours and Regional Brain Dopamine Release in the Rat Using Intracerebral Dialysis. *Brain Res.* **401,** 322-330.

Sossin, W. S. and Scheller, R. H. (1989) A Bag Cell Neuron-Specific Antigen Localizes to a Subset of Dense Core Vesicles in *Aplysia californica*. *Brain Res.* **494,** 205-214.

Starke, K. (1977) Regulation of Noradrenaline Release by Presynaptic Receptor Systems. *Rev. Physiol. Biochem. Pharmacol.* **77,** 1-124.

Starke, K. (1981) Presynaptic Receptors. *Ann. Rev. Pharmacol. Toxicol.* **21,** 7-30.

Sulzer, D. and Rayport, S. (1990) Amphetamine and Other Psychostimulants Reduce pH Gradients in Midbrain Dopaminergic Neurons and Chromaffin Granules: A Mechanism of Action. *Neuron* **5,** 797-808.

Sulzer, D., Chen, T.-K., Lau, Y. Y., St. Remy, C., Kristensen, H., Ewing, A. G., and Rayport, S. (1994) Amphetamine Redistributes Dopamine from Synaptic Vesicles to the Cytosol and Promotes Reverse Transport. submitted to *Neuron.*

Sulzer, D., Maidment, N. T., and Rayport, S. (1993) Amphetamine and Other Weak Bases Act to Promote Reverse Transport of Dopamine in Ventral Midbrain Neurons. *J. Neurochem.* **60,** 527-535.

Tank, D. W., Sugimori, M., Connor, J. A., and R. R. Llinas (1988) Spatially Resolved Calcium Dynamics of Mammalian Purkinje Cells in Cerebellar Slice. *Science* **242,** 773-776.

Thomas, L., Hartung, K., Langosch, D., Rehm, H., Bamberg, E., Franke, W. W., and Betz, H. (1988) Identification of Synaptophysin as a Hexameric Channel Protein of the Synaptic Vesicle Membrane *Science* **242,** 1050-1053.

Thomas, R. C. and Moody, W. J. (1980) Ion-Sensitive Microelectrodes for Intracellular Use. *Trends Biochem. Sci.* **5,** 86-87.

Trifarro, J. M. and Lee, R. W. H. (1980) Morphological Characteristics and Stimulus-Secretion Coupling in Bovine Adrenal Chromaffin Cell Cultures. *Neurosci.* **5,** 1533-1546.

Wagner, J. A. (1985) Structure of Catecholamine Secretory Vesicles from PC12 Cells. *J. Neurochem.* **45,** 1244-1253.

Westfall, T. C. (1977) Local Regulation of Adrenergic Neurotransmission. *Physiol. Rev.* **57,** 659-728.

Wightman, R. M. (1981) Microvoltammetric Electrodes. *Anal. Chem.* **53,** 1125A-1134A.

Wightman, R. M. (1988) Voltammetry with Microscopic Electrodes in New Domains. *Science* **240,** 415-420.

Wightman, R. M. and Wipf, D. O. (1988) Voltammetry at Ultramicroelectrodes. in *Electroanalytical Chemistry* (Bard, A. J., ed.) pp. 267-353, Marcel Dekker, NY.

Wightman, R. M., Jankowski, J. A., Kennedy, R. T., Kawagoe, K. T., Schroeder, T. J., Leszczyszyn, D. J., Near, J. A., Diliberto, Jr., E. J., and Viveros, O. H. (1991) Temporally Resolved Catecholamine Spikes Correspond to Single Vesicles Release from Individual Chromaffin Cells. *Proc. Natl. Acad. Sci. U.S.A.* **88,** 10754-10758.

Winkler, H. and Westhead, E. (1980) The Molecular Organization of Adrenal Chromaffin Granules. *Neurosci.* **5,** 1803-1823.

Wise, R. A. and Bozarth, M. A. (1987) Brain Mechanisms of Drug Reward and Cuphoria. *Psych. Med.* **3,** 445-460.

Yoo, S. H. and Lewis, M. S. (1992) Effects of pH and Ca^{2+} on Monomer-Dimer and Monomer-Tetramer Equilibria of Chromogranin A. *J. Biol. Chem.* **267,** 11236-11241.

Zaczek, R., Culp, S., and DeSouza, E. B. (1991) Interactions of [^{3}H]amphetamine With Rat Brain Synaptosomes. II. Active Transport. *J. Pharmacol. Exp. Ther.* **257,** 830-835.

Zetterström, T., Sharp, T., Marsden, C. A., and Ungerstedt, U. (1983) In Vivo Measurement of Dopamine and Its Metabolites by Intracerebral Dialysis: Changes After d-Amphetamine. *J. Neurochem.* **41,** 1769-1773.

Zhou, R., Luo, G., and Ewing, A. G. (1994) Direct Observation of the Effect of Autoreceptors on Stimulated Release of Catecholamines from Adrenal Cells. *J. Neurosci.* **14,** 2402-2407.

FIGURE CAPTIONS

Figure 1 Differential pulse voltammograms from artificial sea water (ASW) (A) and from 2 living metacerebral cells (B-C and D-F). In the first experiment (B, C) the endogenous peak at +530 mV was increased by ionophoretic intracellular injection of 5-HT from 0.76 to 1.62 mM. In the second experiment (D-F), the cerebral ganglion was superfused by a 5 mM solution of L-tryptophan (Trp) in ASW. With time, L-tryptophan accumulated inside the neurone (peak at +1000 mV) and induced a synthesis of 5-HT as manifested by the increase of the peak at +530 mV. The intracellular concentrations of 5-HT and tryptophan were 0.20 and 0.09 mM at 5 min, 0.44 and 0.41 mM at 15 min, 0.74 and 1.06 mM at 30 min, respectively (With permission from Meulemans et al. 1987).

Figure 2. Increase of intracellular 5-HT concentration due to stimulation. The two metacerebral cells of one ganglion were successively impaled with the same platinum microelectrode. Upper graph: the soma was directly stimulated by an intracellular 3 M KCL microelectrode (S: 3 Hz for 70 and 150 s). Lower graph: the cell was depolarized from -51 mV to -27 mV by bath application of 100 mM KCL for 15 min. (With permission from Meuelmans et al. 1987).

Figure 3. Schematic of the brain of *Planorbis corneus* showing electrode placement and microinjector relative to the giant dopamine cell (GDC). (With permission from Chien et al. 1988).

Figure 4. Effect of 700 µl of 0.6 mM nomifensine on repeated dopamine bathings (50 µL; 0.5 mM): before (●) and after (O) nomifensine application. The oxidation current was monitored at 0.78 V versus a sodium-saturated calomel reference electrode with 7 s between measurements. (With permission from Chien et al. 1990).

Figure 5. Intracellular injection of DA induces reverse transport. (A) Intracellular injection of 4 pL of 0.5 mM DA (arrows) induced reliable increases in extracellular DA release. During extracellular perfusion with 10 µM nomifensine (dashed line) the same DA injections were markedly attenuated. Perfusion of nomifensine-containing medium and its replacement by control medium produced current spikes (asterisks). Data have been baseline corrected by subtracting the curve fit to the background signal. (B) Background subtracted voltammograms (-0.2 to 0.8 V) for the first (—) and second (--), and fourth (···) intracellular DA injections shown in (A). The voltammograms monitored at the face of the neuron were nearly identical to DA. All three voltammograms were sigmoidal with a half-wave potential of approximately 0.2 V. (With permission from Sulzer et al. 1994).

Figure 6. (A) AMPH (8 pL of 100 mM) was injected intracellularly (arrow). The increase in extracellular DA was measured by oxidation current with a 2 µm carbon ring ultramicroelectrode. The electrode was touching the GDC membrane and held at a steady potential of 0.8 V. (B) The shape of the voltammogram (-0.2 to 0.8 V) taken at the peak current value 14 s post

injection (filled circles) closely matched the voltammogram for a DA standard (solid line). Calibration: i = 0.5 for the experiment and 31.5 for the standard. (With permission from Sulzer et al. 1994).

Figure 7. Experimental arrangement for measuring secretion from single adrenal medullary chromaffin cells. Drawing is approximately to scale. (With permission from Leszczyszyn et al. 1990).

Figure 8. Cyclic voltammetric response (200 V s^{-1}, repeated at 100-ms intervals) of a carbon fiber electrode to norepinephrine ejection from an adjacent micropipette and to catecholamine secretion from a single chromaffin cell. Panels A and B are averaged background-subtracted voltammograms of the substances whose concentration changed during the measurement interval of panels C and D. Each time point in panels C and D is the integrated current recorded from 0.5-0.6 V from individual voltammograms (hatched lines in panels A and B); bars to the right in panels C and D are the conversion of current to catecholamine concentration based on calibration curves constructed with standards. A, C, electrode response to 1-s 3-nL ejection of 20 μM norepinephrine applied at t = 0 with the ejection pipette 20 μm from the electrode. B, D, electrochemical response obtained with the electrode tip adjacent to a single cell; at t = 0, a 1-s ejection of nicotine (100 μM) was made 20 μm away from the cell. (With permission from Leszczyszyn et al. 1990).

Figure 9. Frequency distribution of individual spike areas determined for various secretagogues. The spikes were measured over a 30-s segment beginning at

the half-rise time. The bins are divided into 0.2-pC intervals. (A) Spike distribution during exposure to ten 3-s, 60 mM K^+ exposures (136 spikes; the balanced salt solution in the ejection pipette contained 90 mM Na^+ and 60 mM K^+). (B) Spike distribution during 7 exposures to 1 mM carbamoylcholine simulations (137 spikes). (C) Spike distribution during 10 exposures to 10 μM nicotine (80 spikes). (D) Spike distribution during 10 exposures to 100 μM nicotine (211 spikes). (With permission from Wightman et al. 1991).

Figure 10. Secretion of epinephrine from an individual adrenal cell. (A) Current versus time profile of single cell response to 100 μM nicotine introduced at 0 s: oxidative current (solid line), reductive current (dotted line), adrenochrome current (dashed line), current at 0 V (dashed-dotted line). (B) E_p (solid line), ΔE_p (dotted line), and i_{cyc}/i_{ox} (dashed line) versus time. The scale for each of these parameters is adjusted so that the values will fall between the limits of pure epinephrine (upper dashed line) and pure norepinephrine (lower dashed line) as determined by the postcalibrations. (C) Background-subtracted cyclic voltammogram (solid line) taken at the asterisk in (A). Circles represent the background-subtracted cyclic voltammogram of the epinephrine postcalibration. Voltammograms have been normalized to the oxidative peak currents. (With permission from Ciolkowski et al. 1992).

Figure 11. Secretion of norepinephrine from an individual adrenal cell. The parameters for (A) and (B) are the same as those for Figure 10. (C) is the same as Figure 10, except circles represent the background-subtracted cyclic voltammogram

of the norepinephrine post-calibration. (With permission from Ciolkowski et al. 1992).

Figure 12. Electrochemical detection of secretion from single vesicles. (A) Examples of signals recorded by the amperometric constant-voltage method. The voltage protocol is shown in the bottom trace, and representative amperometric current signals are shown above, aligned in time relative to the stimulating pulse. The signals vary in amplitude and duration, and occasionally there are "failures" (sweeps without a response). (B) Response to steady-state depolarization to 0 mV after the recording of part (A) (note difference in time scales). (With permission from Chow et al. 1992).

Figure 13. Rising phase of amperometric current transients cannot be explained by instantaneous release of secretory vesicle contents. (A) Single amperometric current transients at high resolution. Note that the fast rising phase in two out of the three examples is preceded by a small pedestal or "foot" (arrows). Such "foot" signals precede most of the transients with a fast rise time. The "foot" signals were typically much smaller than the average signal. (B) Histogram of duration of "foot" signals. Data from three cells are pooled, where 84 large (>20 pA) and fast (rise time <3 ms) signals were counted. 75 of those were preceded by a discernible "foot". The number of occurrences is plotted against the duration of the "foot", as defined in (A). The mean of "foot" durations was 8.26 ms. (C) Histogram of "foot" charges. The same "foot" signals as those of (B) were integrated to calculate the charge involved. Mean charge:

34 fC or 1.05 x 10^5 molecules. The mean amplitude of the "foot" signal was 7.17 ± 5.28 pA (mean ± s.d.). (With permission from Chow et al. 1992).

Figure 14. Effect of piperoxan (20 μM) on nicotine induced exocytosis of catecholamines. (A) a, g: 3-s application of 100 μM nicotine, b, c, d, e, f: 5-s application of 20 μM piperoxan. (B) a, c: 3-s application of 100 μM nicotine. b: 5-s application of balanced salt solution. Electrode potential: 650 mV vs SSCE. (With permission from Zhou et al. 1994).

Figure 15. Amperometric response of a carbon fiber electrode placed at a single chromaffin cell following a 3-s application of 100 μM nicotine (a), and a 5-s application of 20 μM amphetamine (b). (With permission from Zhou et al. 1994).

Figure 16. Amperograms of single vesicular exocytosis from PC12 cells. (A) Amperogram of a control experiment with no cell near the tip of the working electrode. (B) Amperogram of vesicular exocytosis induced by 1 mM nicotine in 105 mM K^+ balanced salt solution. (C) Enlargement of a one second period of the amperogram from the first stimulation. Data displayed correspond to the time period near the middle of the first base line disturbance in (B). (With permission from Chen et al. 1994b).

Figure 17. Frequency distribution of quantal size from PC12 cells. The bins are divided into 66 z-mole (40,000 molecules) intervals. Numbers on the x-axis represent the mean of each interval. Data shown here were obtained from the first

stimulation of 13 individual cells 1,912 spikes are included. (With permission from Chen et al. 1994b).

Figure 18. Amphetamine exposure decreases the quantal amplitude of individual release events from PC12 cells. Representative electrochemical records of quantal release (selected randomly) for a control cell (A) and a cell that has been incubated in 10 μM d-amphetamine for 10 min (B). Cells were stimulated by local perfusion (30 nL of 1 mM nicotine in 105 mM KCL saline) to induce vesicular exocytosis. Amphetamine decreased the average quantal amplitude to 48% ± 5.4% of control. (With permission from Sulzer et al. 1994).

Figure 19. Quantal release detected from the cell body of the dopamine neuron of *Planorbis corneus*. (A) is a schematic of the cell body, an intracellular pipette for injecting Ringer solution to the cell and a carbon fiber electrode placed close to the penetrating site. (B) is a typical response observed following intracellular stimulation with sodium chloride. A 30 pL of Ringer solution was injected at the arrow position and transient quantal events were elicited about 5 s after injection. (With permission from Chen et al. 1994a).

Figure 20. Fast scan voltammograms of dopamine. Background substrated voltammograms were obtained from dopamine ejection (top graph) and during quantal release of dopamine at cell surface (bottom graph) with a carbon ring electrode (scan rate 300 V s^{-1}, 2 ms delay between each scan). (With permission from Chen et al. 1994a).

Figure 21. Frequency distribution of spike areas from the dopamine neuron of *Planorbis corneus*. The area of transient events is displayed in units of charge (fC). The average content is about 0.5 ± 0.2 attomole (300,000 molecules) per vesicle. (With permission from Chen et al. 1994a).

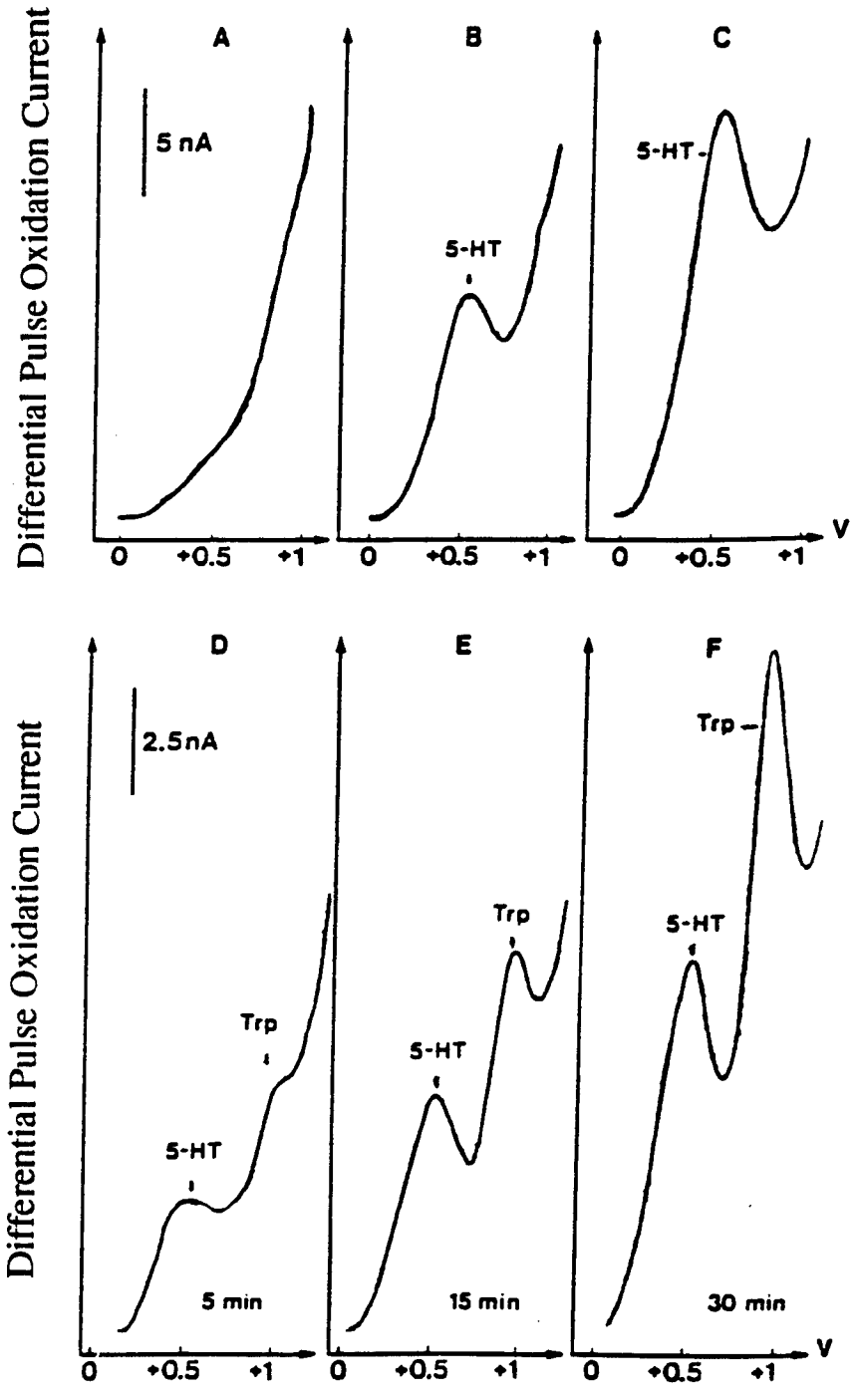
Differential Pulse Oxidation Current
A
B
C
5 nA
5-HT
5-HT
0
+0.5
+1
V
Differential Pulse Oxidation Current
D
E
F
2.5nA
Trp
5-HT
Trp
5-HT
Trp
5-HT
5 min
15 min
30 min
0
+0.5
+1
V

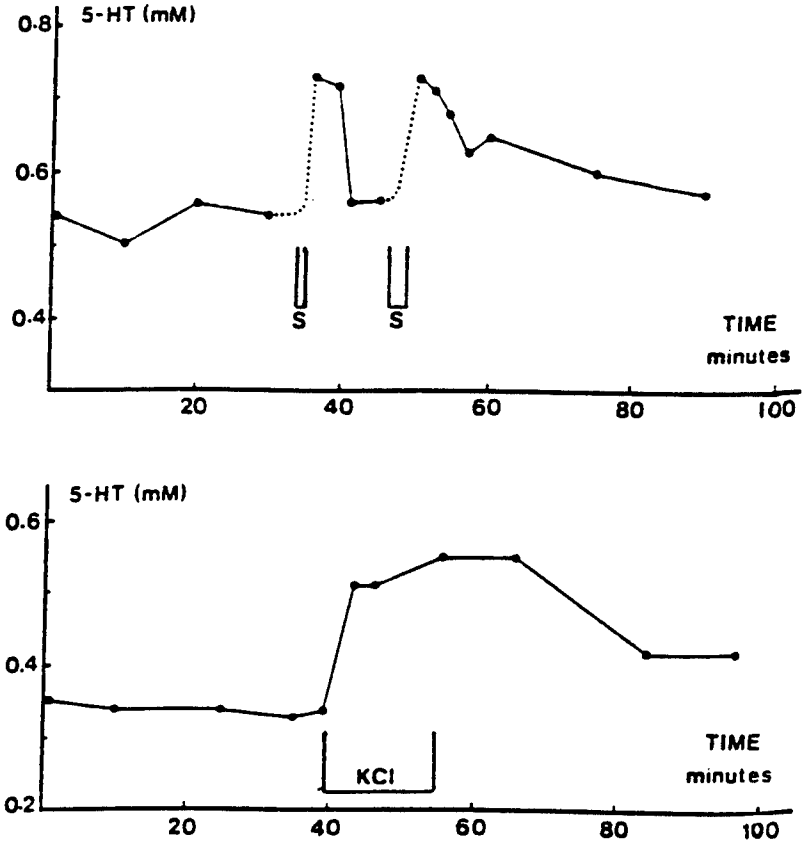
5-HT (mM)
0.8
0.6
0.4
S
S
TIME
minutes
20
40
60
80
100
5-HT (mM)
0.6
0.4
0.2
KCl
TIME
minutes
20
40
60
80
100

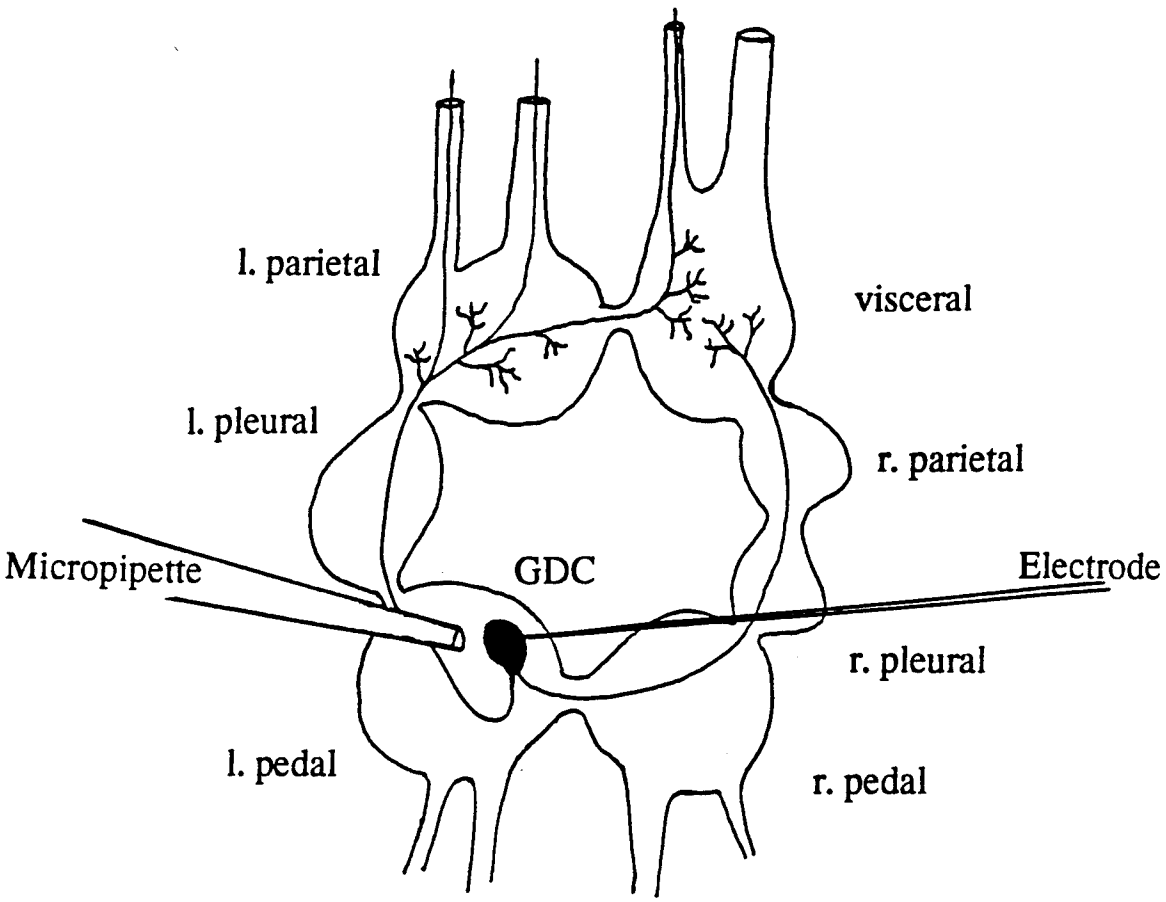
l. parietal
visceral
l. pleural
r. parietal
Micropipette
GDC
Electrode
r. pleural
l. pedal
r. pedal

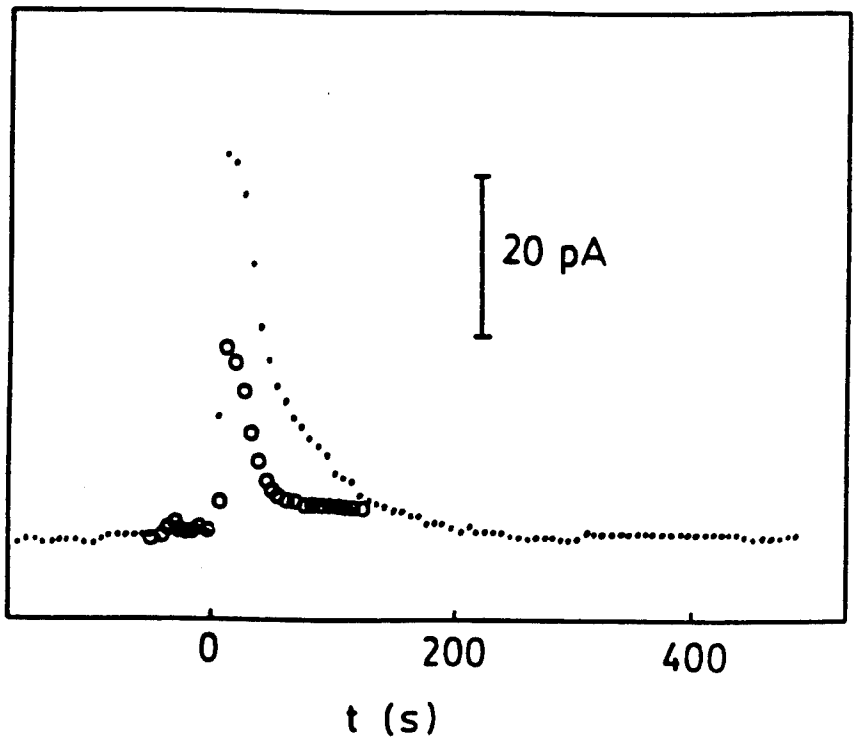
20 pA
0
200
400
t (s)

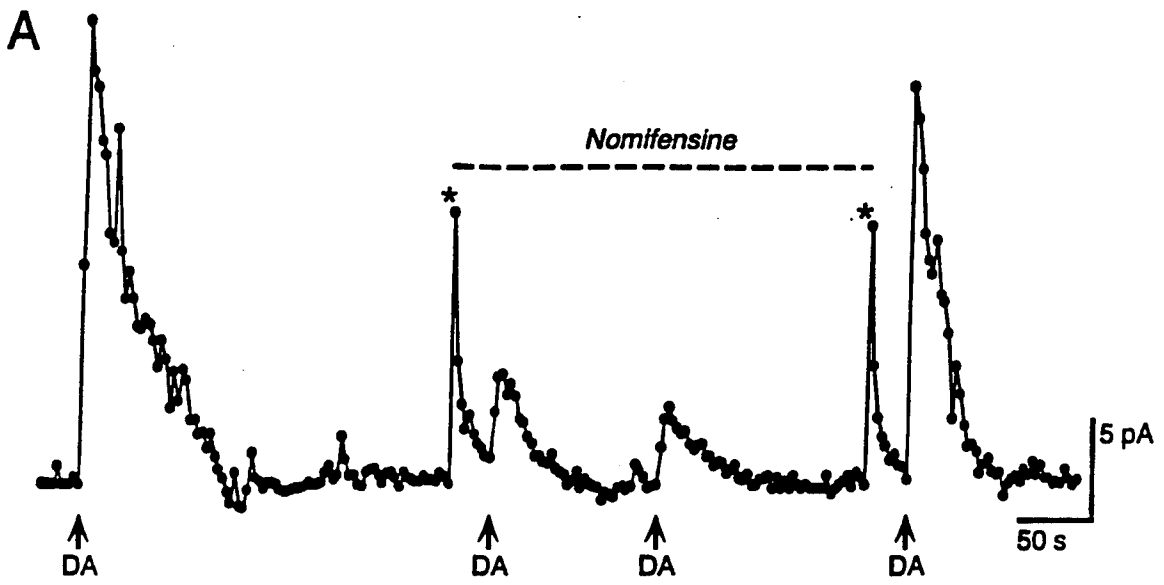
A
Nomifensine
*
*
5 pA
50 s
DA
DA
DA
DA

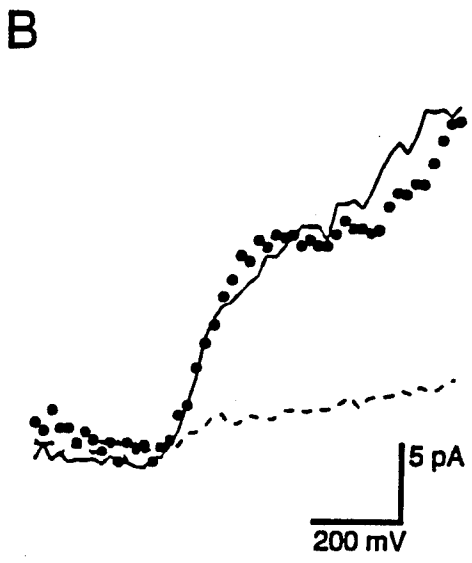
B
5 pA
200 mV

A

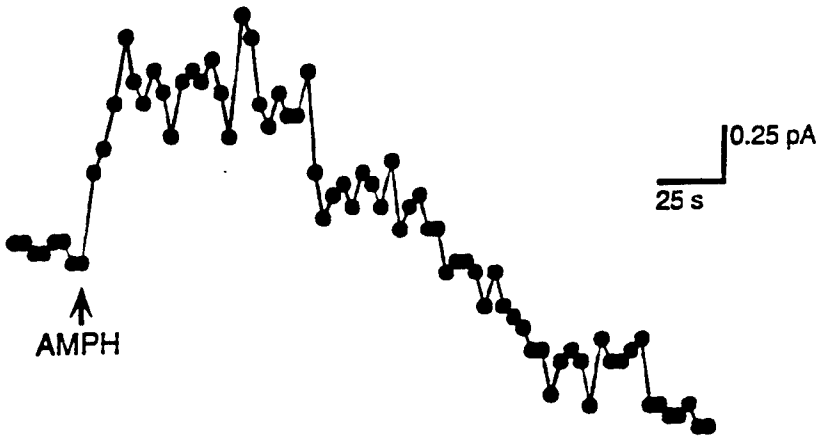

B

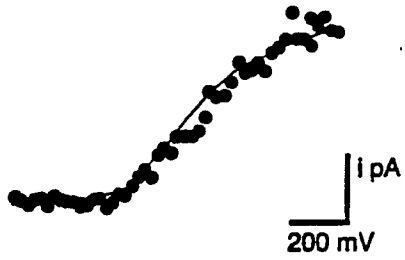

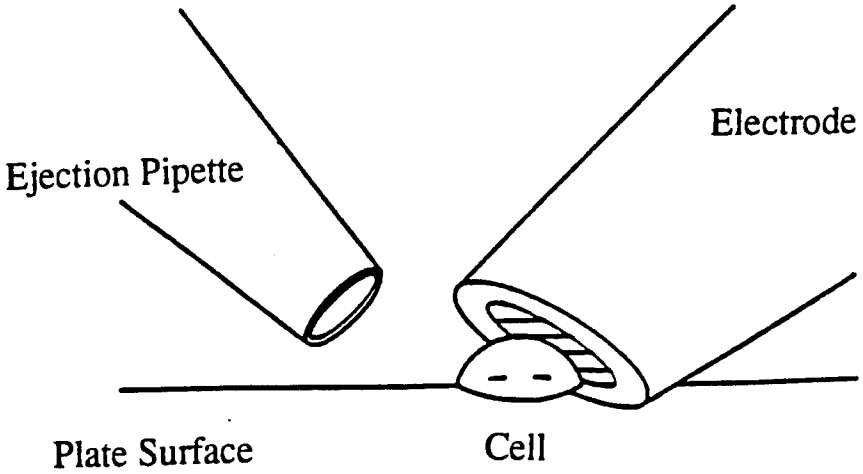
Electrode
Ejection Pipette
Plate Surface
Cell

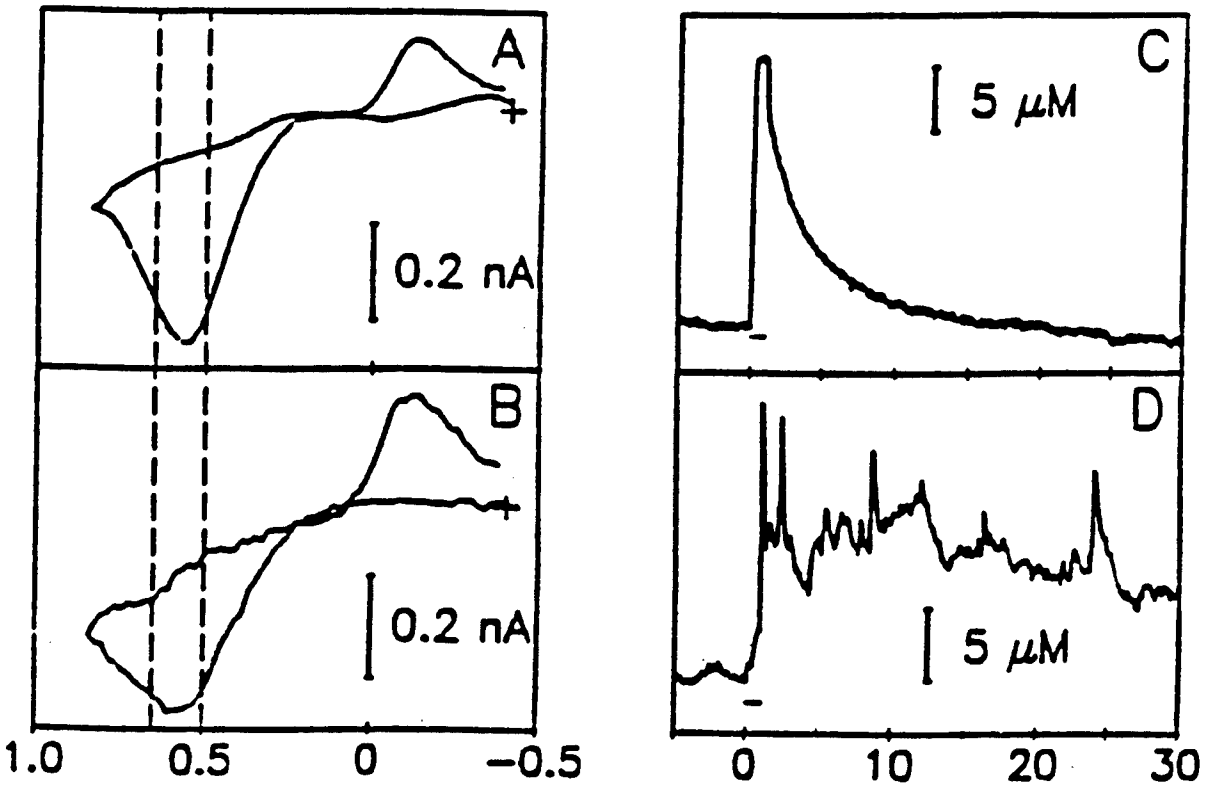
A
0.2 nA
B
0.2 nA
1.0
0.5
0
−0.5
E (V vs SSCE)
C
5 μM
D
5 μM
0
10
20
30
Time (s)

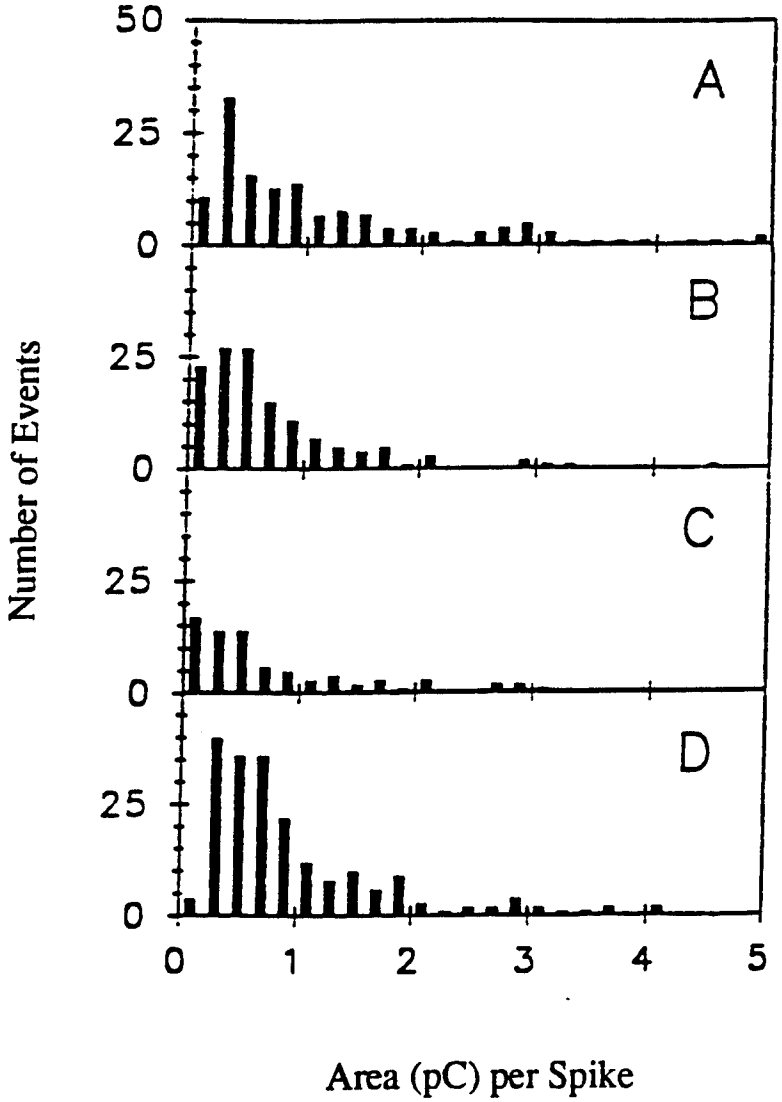
50
25
0
A
25
0
B
25
0
C
25
0
D
0
1
2
3
4
5
Number of Events
Area (pC) per Spike

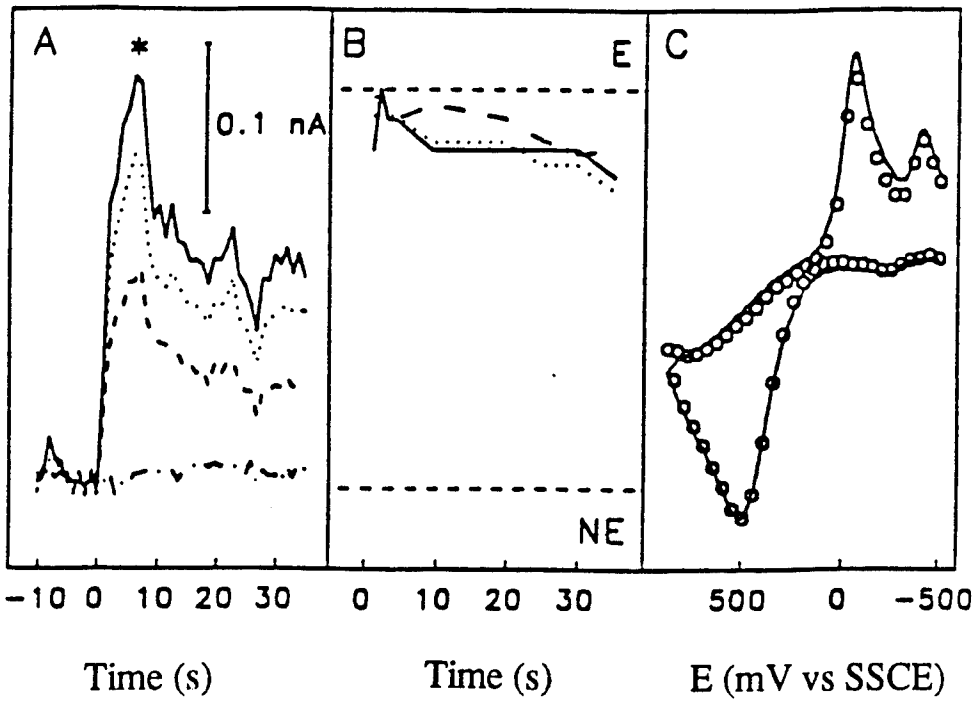
A
*
0.1 nA
B
E
NE
C
−10 0 10 20 30
0 10 20 30
500 0 −500
Time (s)
Time (s)
E (mV vs SSCE)

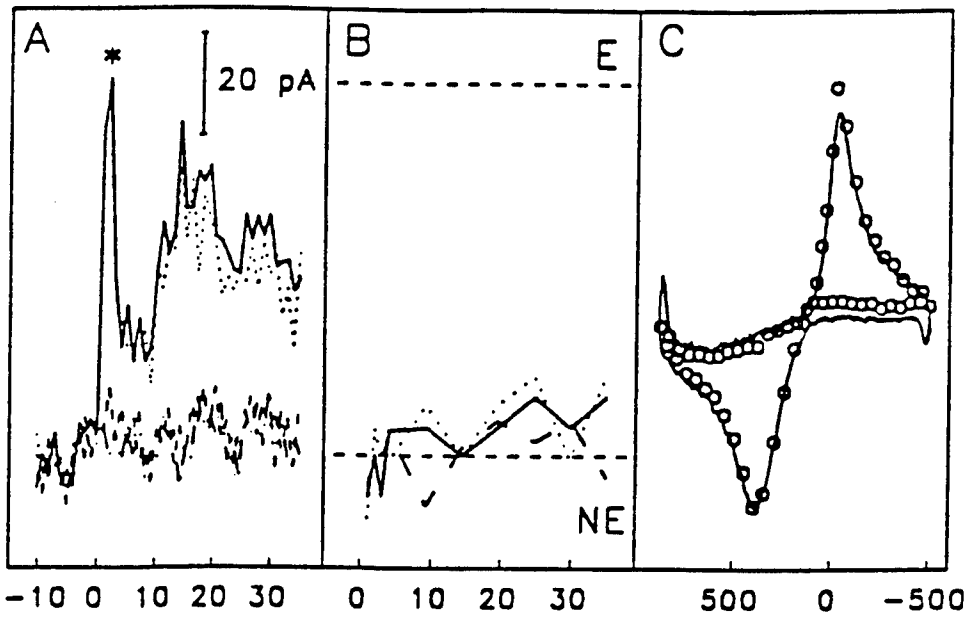
A
B
C
20 pA
E
NE
−10 0 10 20 30
0 10 20 30
500 0 −500
Time (s)
Time (s)
E (mV vs SSCE)

A

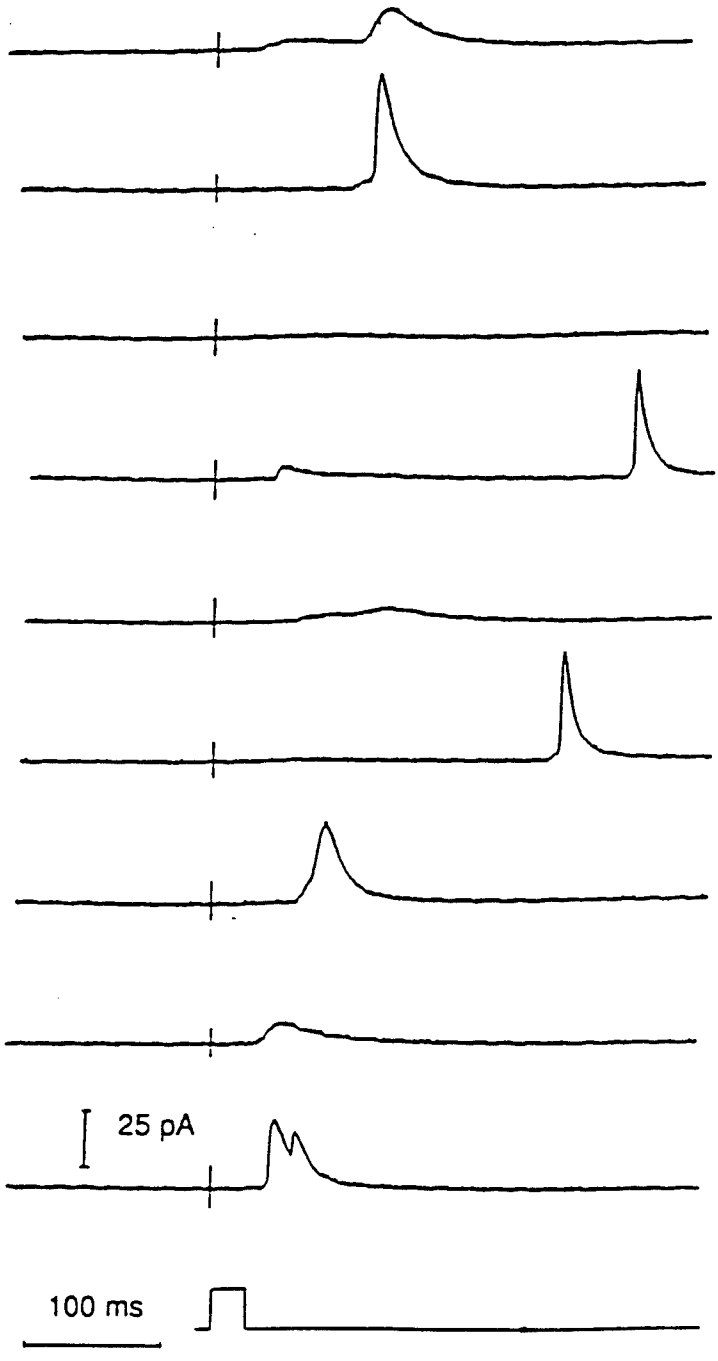

B

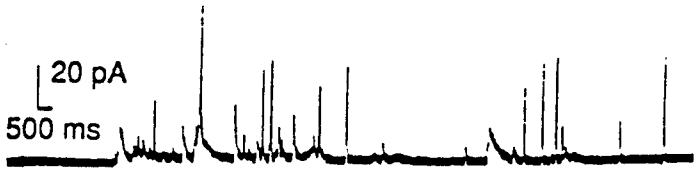

A

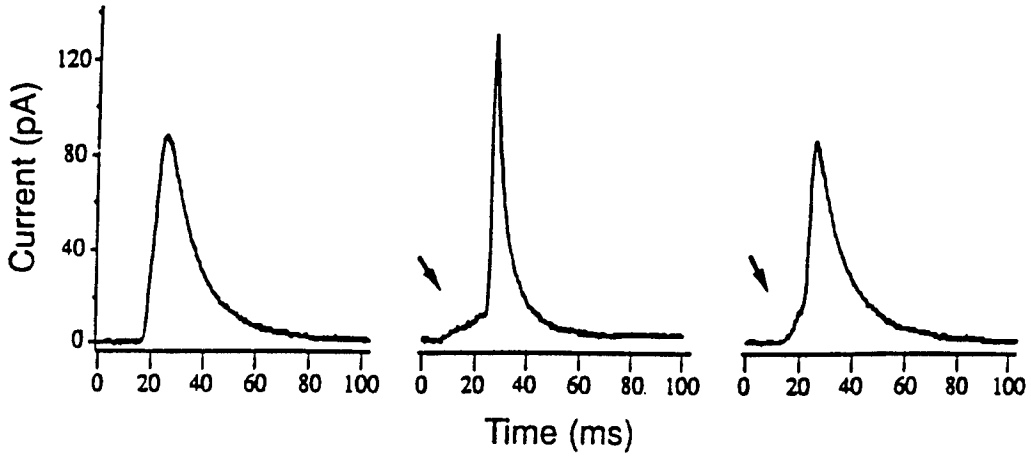
Current (pA)
120
80
40
0
0 20 40 60 80 100
0 20 40 60 80 100
0 20 40 60 80 100
Time (ms)

B

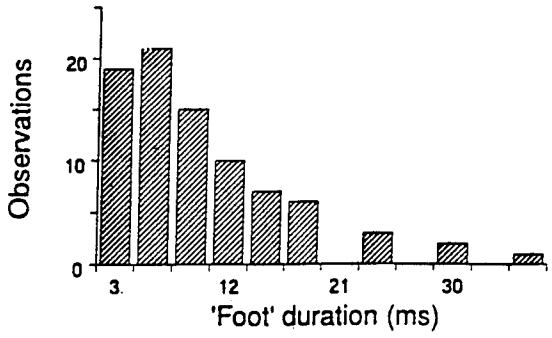
Observations
20
10
0
3
12
21
30
'Foot' duration (ms)

C

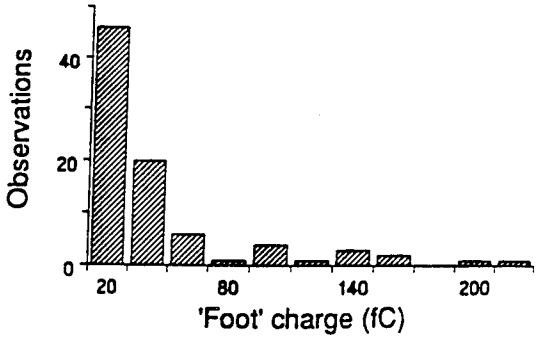
Observations
40
20
0
20
80
140
200
'Foot' charge (fC)

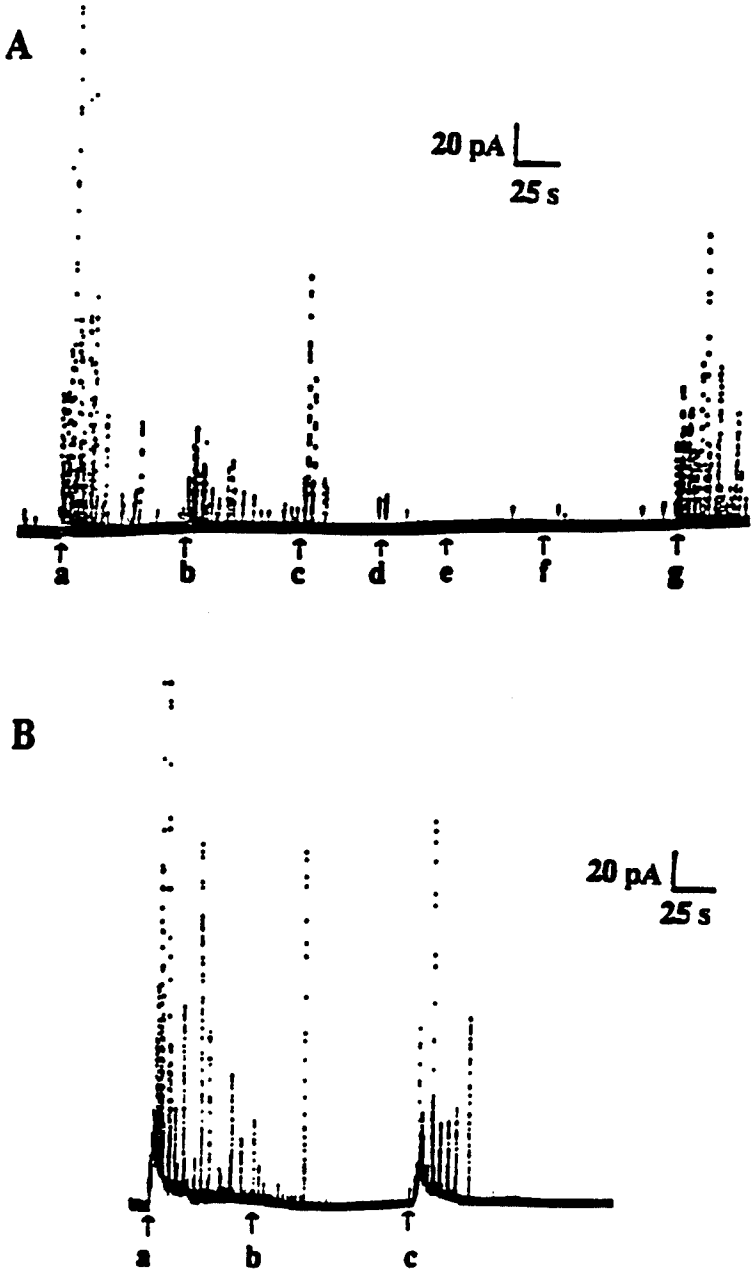
A
20 pA
25 s
a
b
c
d
e
f
g
B
20 pA
25 s
a
b
c

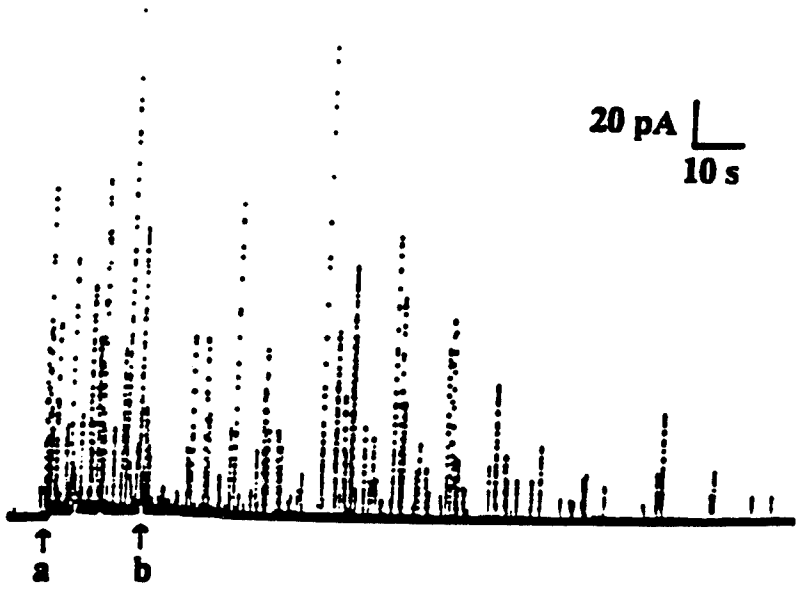
20 pA
10 s
a
b

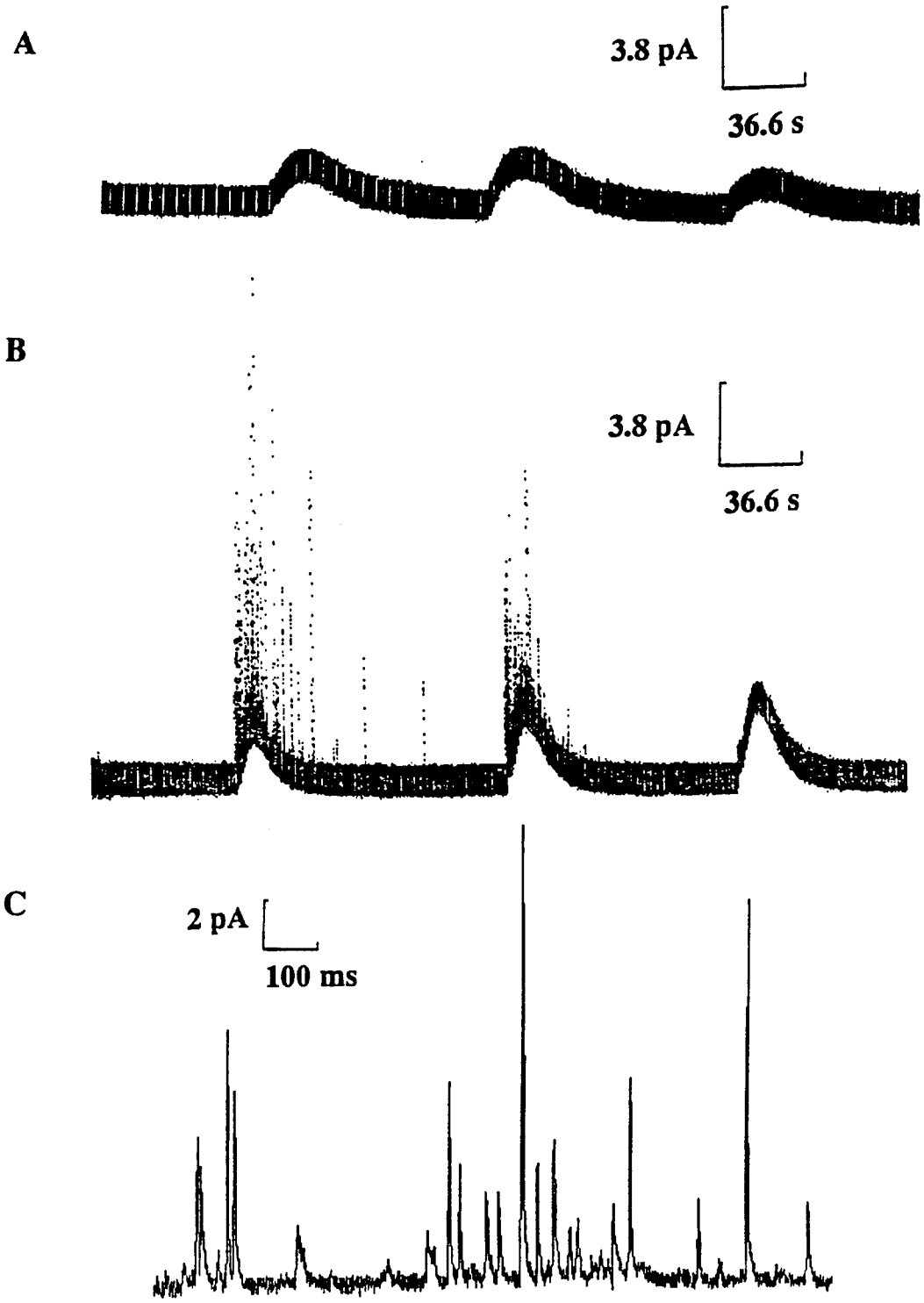
A
3.8 pA
36.6 s
B
3.8 pA
36.6 s
C
2 pA
100 ms

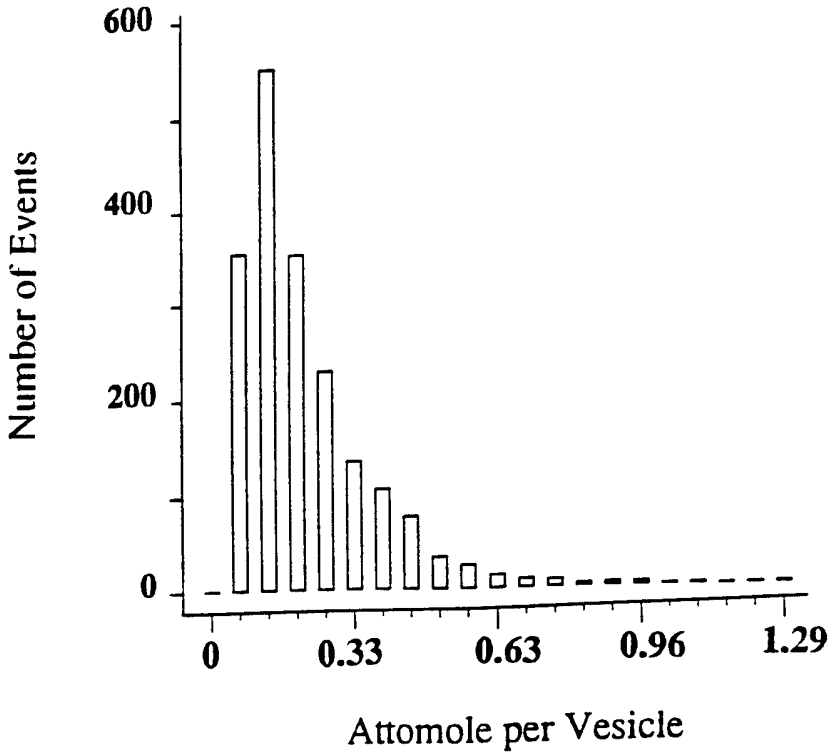
600
400
200
0
Number of Events
0
0.33
0.63
0.96
1.29
Attomole per Vesicle

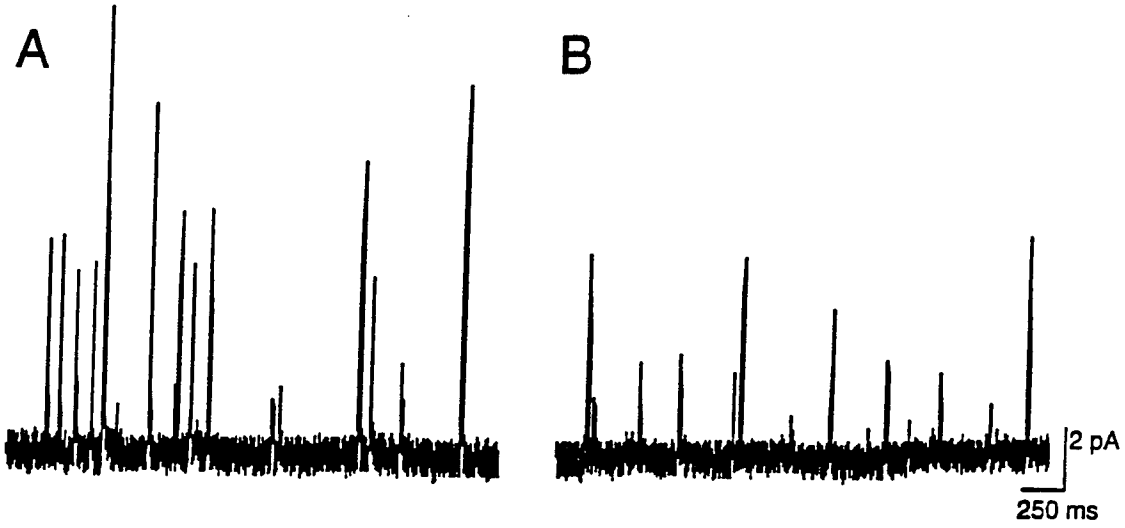
A
B
2 pA
250 ms

A

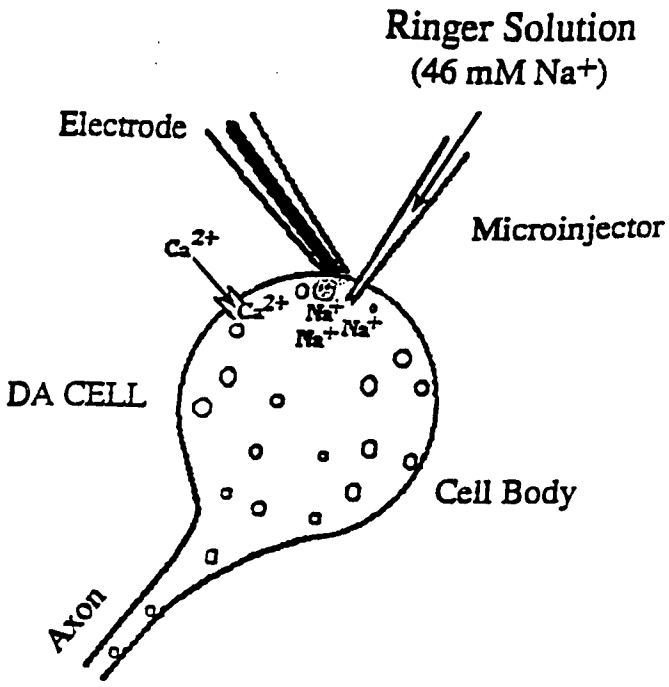
Ringer Solution
(46 mM Na+)
Electrode
Microinjector
Ca2+
Ca2+
Na+
Na+
Na+
DA CELL
Cell Body
Axon

B

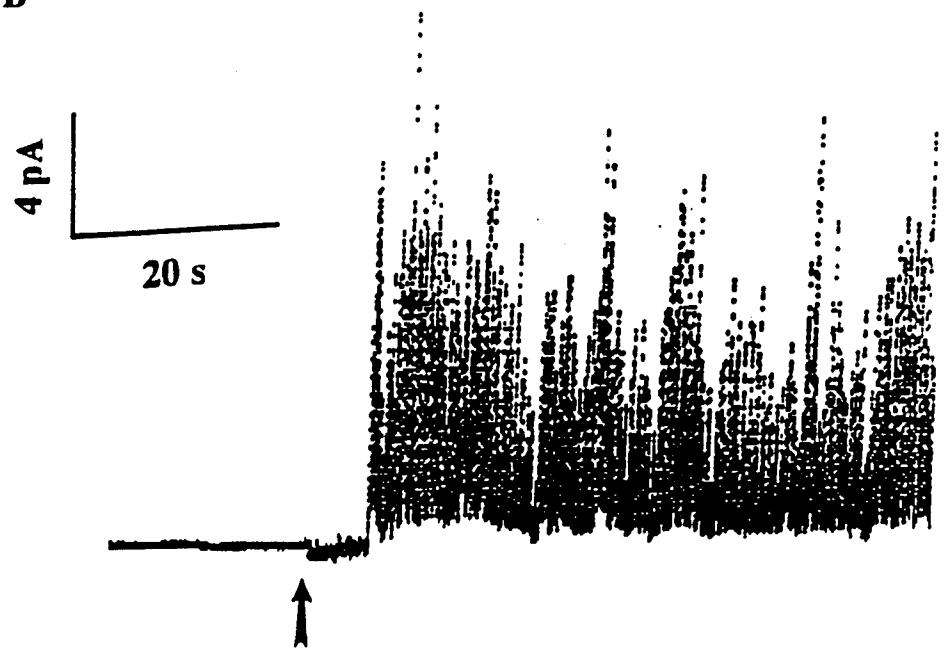
4 pA
20 s

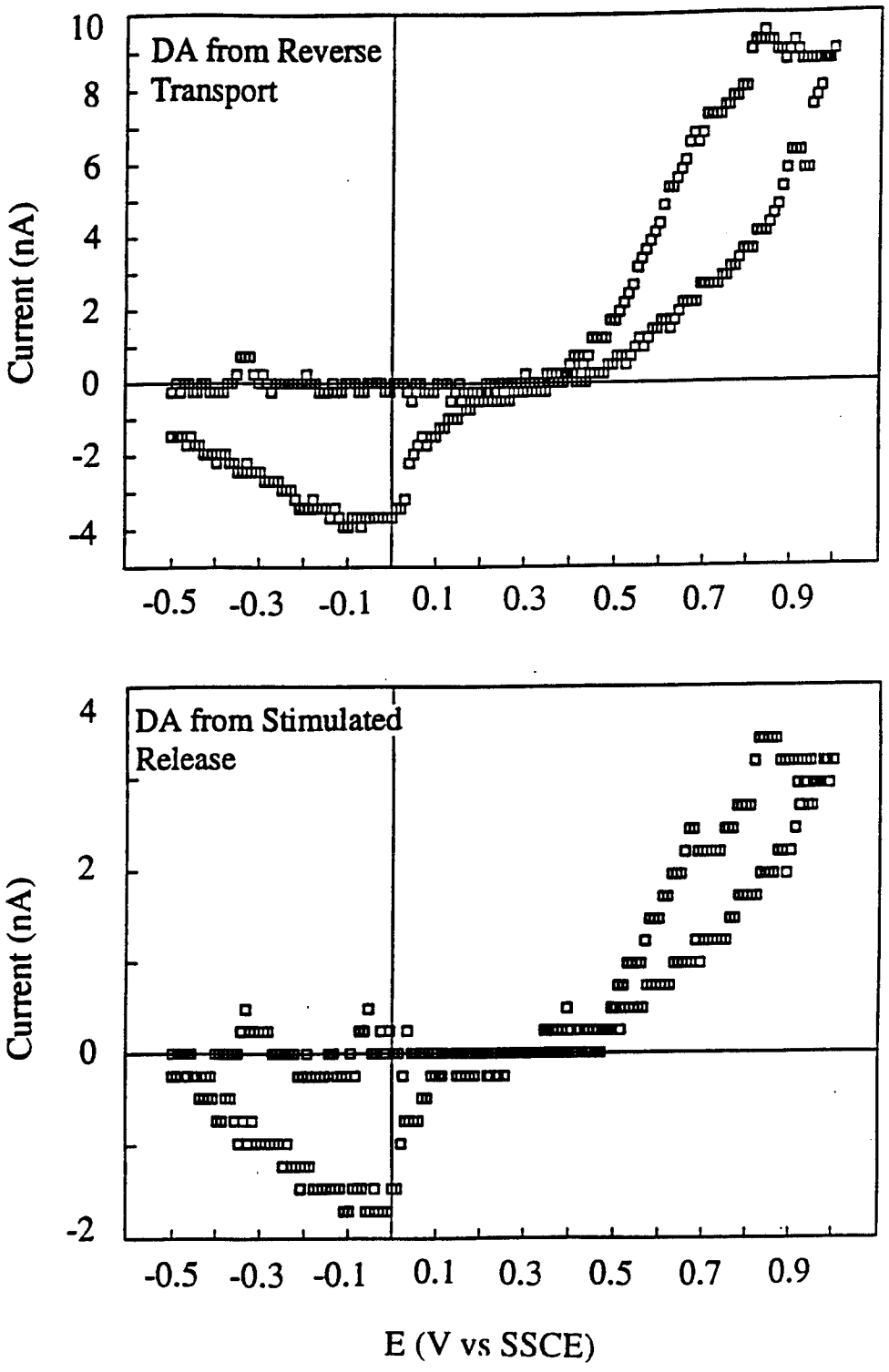
DA from Reverse Transport
Current (nA)
10
8
6
4
2
0
-2
-4
-0.5
-0.3
-0.1
0.1
0.3
0.5
0.7
0.9
DA from Stimulated Release
Current (nA)
4
2
0
-2
-0.5
-0.3
-0.1
0.1
0.3
0.5
0.7
0.9
E (V vs SSCE)

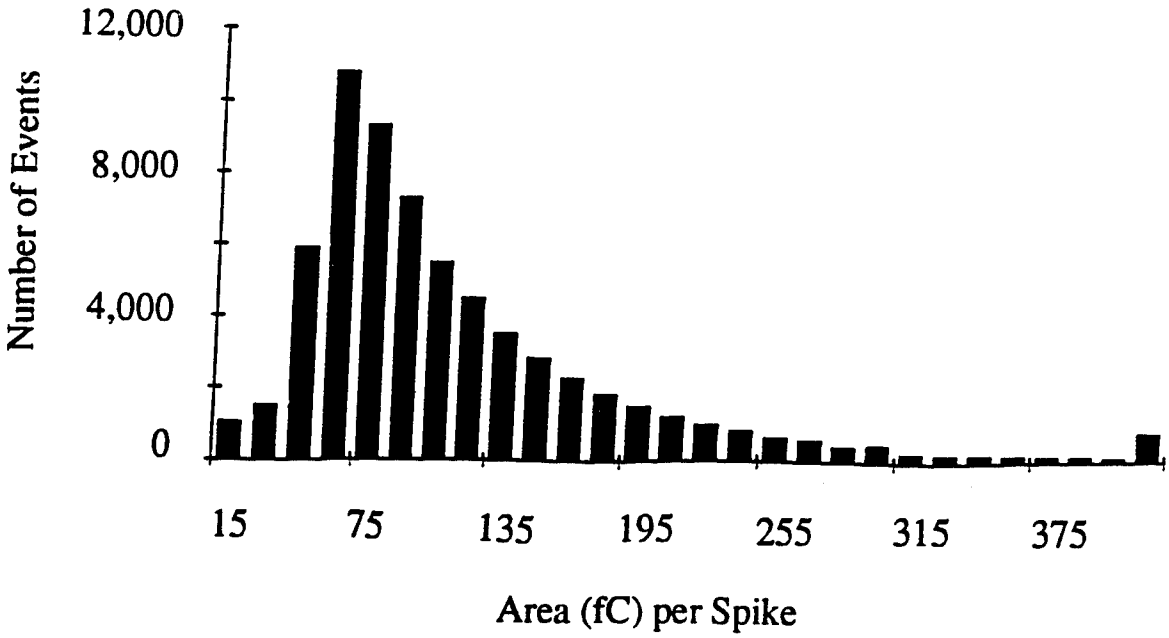
12,000
8,000
4,000
0
Number of Events
15
75
135
195
255
315
375
Area (fC) per Spike